DOI: 10.1534/genetics.106.057596

ELM1 Is Required for Multidrug Resistance in *Saccharomyces cerevisiae*

Abdul-Kader Souid,*[,1] Chen Gao,[†,1] Luming Wang,[†,1] Elena Milgrom[†,1] and W.-C. Winston Shen[†,2]

[†]*Department of Biochemistry and Molecular Biology and* **Department of Pediatrics, State University of New York Upstate Medical University, Syracuse, New York 13210*

Manuscript received February 24, 2006
Accepted for publication May 30, 2006

ABSTRACT

In *Saccharomyces cerevisiae*, transcription of several drug transporter genes, including the major transporter gene *PDR5*, has been shown to peak during mitosis. The significance of this observation, however, remains unclear. *PDR1* encodes the primary transcription activator of multiple drug transporter genes in *S. cerevisiae*, including *PDR5*. Here, we show that in synchronized *PDR1* and *pdr1-3* (multidrug resistant) strains, cellular efflux of a known substrate of ATP-binding-cassette transporters, doxorubicin (a fluorescent anticancer drug), is highest during mitosis when *PDR5* transcription peaks. A genetic screen performed to identify regulators of multidrug resistance revealed that a truncation mutation in *ELM1* (*elm1-300*) suppressed the multidrug resistance of *pdr1-3*. *ELM1* encodes a serine/threonine protein kinase required for proper regulation of multiple cellular kinases, including those involved in mitosis, cytokinesis, and cellular morphogenesis. *elm1-300* as well as *elm1*Δ mutations in a *pdr1-3* strain also caused elongated bud morphology (indicating a G_2/M delay) and reduction of *PDR5* transcription under induced and noninduced conditions. Interestingly, mutations in several genes functionally related to *ELM1*, including c*la4*Δ, *gin4*Δ, and *cdc28-C127Y*, also caused drastic reductions in drug resistance and *PDR5* transcription. Collectively, these data show that *ELM1*, and genes encoding related serine/threonine protein kinases, are required for regulation of multidrug resistance involving, at least in part, control of *PDR5* transcription.

In *Saccharomyces cerevisiae*, transcriptional upregulation of transporters that belong to the ATP-binding-cassette (ABC) superfamily results in multiple drug resistance or in pleiotropic drug resistance (PDR). Transcriptional activation of many of these transporters is known to occur with drug exposure (*e.g.*, cycloheximide) or in the presence of gain-of-function mutations in the transcriptional activators themselves (Balzi and Goffeau 1995; Wolfger *et al.* 2001; Moye-Rowley 2003). Transcription of most genes is known to be significantly reduced during mitosis, and this mitotic repression has been, at least in part, attributed to inactivation of the transcriptional machinery (Gottesfeld and Forbes 1997; Long *et al.* 1998). Surprisingly, microarray analysis indicates that transcription of several drug transporter genes, including *PDR5*, peaks during mitosis (Spellman *et al.* 1998; reviewed in Bahler 2005; Wittenberg and Reed 2005). However, this finding has not been thoroughly investigated, and the impact of *PDR5* transcriptional upregulation during mitosis on multidrug resistance remains unknown.

Two major transcriptional activators, Pdr1 and Pdr3, control the level of many drug transporters in *S. cerevisiae* (Gao *et al.* 2004; Milgrom *et al.* 2005 and references therein). These homologous proteins belong to the Gal4 superfamily with Cys_6-Zn(II) DNA-binding domains (Poch 1997; Kolaczkowski *et al.* 1998; Bauer *et al.* 1999). The DNA-binding domain of Pdr1 targets over a dozen transport gene promoters (most notably *PDR5*) with the pleiotropic drug resistance element (PDRE) 5′-TCCGCGGA-3′ (Balzi and Goffeau 1995; Kolaczkowska *et al.* 2002). The functions of Pdr1 and Pdr3 overlap; however, Pdr3, but not Pdr1, is subject to auto-regulation (Delahodde *et al.* 1995). Several substitution mutations within Pdr1 result in a hyperactive activator (*e.g.*, F815S in the Pdr1-3 hyperactivator protein encoded by the *pdr1-3* allele (Meyers *et al.* 1992; Carvajal *et al.* 1997) that increases the transcription of many genes encoding ABC transporters (including *PDR5*), as well as permeases and enzymes involved in lipid and cell-wall synthesis (DeRisi *et al.* 2000). Similarly to Pdr1, several hyperactive Pdr3 activators, including that encoded by the *pdr3-2* allele, were identified (Nourani *et al.* 1997).

The Pdr5 transporter is a major plasma-membrane-associated ATPase regulated by Pdr1/Pdr3, and it is responsible for cellular detoxification of many agents, including the anticancer drug doxorubicin (Rogers *et al.* 2001). Yeast Pdr5 exhibits functional homology to

[1]These authors contributed equally to this work.

[2]*Corresponding author:* Department of Biochemistry and Molecular Biology, State University of New York, Upstate Medical University, 750 E. Adams St., WHA Room 4281, Syracuse, NY 13210.
E-mail: winston.shen@uspto.gov

the mammalian P-glycoproteins (Pgp), and overexpression of Pdr5 confers multidrug resistance. Extensive efforts have been made to identify small molecules that could reverse the drug resistance phenotype, primarily by inhibiting transporter activities (Lewis 2001). In this regard, the function of Pdr5, as well as similar drug transporters of the pathogenic yeast *Candida albicans*, are inhibited by the immunosuppressant FK506 (tacrolimus, Prograf) (Egner *et al.* 1998; Schuetzer-Muehlbauer *et al.* 2003).

We previously characterized the transcriptional regulation of *PDR5* by comparing differences in the recruitment of activators and coactivators and the nucleosome structure in isogenic *PDR1* and *pdr1-3* strains. We demonstrated that Pdr1 is constitutively bound to the *PDR5* promoter. Cycloheximide induction in the wild-type *PDR1* strain alters the nucleosome structure at the *PDR5* upstream activating sequence (UAS) region harboring PDRE. These alternations reflect changes in the interactions between Pdr1 and PDRE and are associated with *PDR5* transcriptional activation (Gao *et al.* 2004). Moreover, we showed that proper interactions between histones and *PDR5* coding sequences specifically require the transcription factor Spt-Ada-Gcn5-acetyltransferase (SAGA) (Milgrom *et al.* 2005). However, factors other than Pdr1 and SAGA that are required for proper transcriptional regulation of *PDR5* remain to be identified.

In *S. cerevisiae*, mitotic entrance is coupled to morphogenesis (Sakchaisri *et al.* 2004). Entry into mitosis is initiated by activation of Clb2-Cdc28/Cdk1 cyclin-dependent kinase (CDK), which involves degradation of its inhibitor Swe1 kinase (McMillan *et al.* 2002). Mechanistically, Swe1 phosphorylation by Cdk1 activates Swe1, and this phosphorylation is required for the formation of a stable Swe1–Cdk1 complex that maintains Cdk1 in an inhibited state (Asano *et al.* 2005; Harvey *et al.* 2005). Additional kinases are involved in the regulation of transition from G_2 to mitosis. *ELM1* (*el*ongated *m*orphology 1) encodes a serine (Ser)/threonine (Thr) protein kinase, and cells harboring *elm1*Δ exhibit elongated filamentous growth, an indication of G_2/M delay (Koehler and Myers 1997). The function of Elm1 kinase in mitotic signaling (Sreenivasan and Kellogg 1999) has been linked, in part, to regulators of septin organization, a key set of protein serine/threonine kinases encoded by *GIN4* and *CLA4*, as well as an interactor of mitotic cyclin Clb2 encoded by *NAP1* (Altman and Kellogg 1997; Benton *et al.* 1997; Carroll *et al.* 1998; Edgington *et al.* 1999; Longtine *et al.* 2000; Gladfelter *et al.* 2004). Support of Elm1 involvement in the G_2/M transition includes the fact that Elm1 is required for hyperphosphorylation of Swe1 during mitosis (Sreenivasan and Kellogg 1999). Elm1 is also required for the regulation of bud emergence at the G_1 phase (Sreenivasan *et al.* 2003). Independently of its roles in the cell cycle, Elm1 appears to function upstream of Snf1, a key AMP-dependent kinase pathway that regulates carbon metabolism in yeast (Hong *et al.* 2003; Sutherland *et al.* 2003) and mammalian cells (Woods *et al.* 2003).

In this study, we show that *PDR5* transcription during cell cycle progression is inversely correlated with cellular accumulation of doxorubicin. A truncation and null mutation in *ELM1* were identified as suppressors of *pdr1-3*. Yeast strains harboring mutations in genes encoding Elm1-related kinases (*e.g.*, *gin4*Δ, c*la4*Δ, and *cdc28-C127Y*) similarly reversed the multidrug resistance of *pdr1-3*, exhibited elongated bud morphology and impaired *PDR5* transcription (without affecting Pdr1-independent transcription) and abolished cellular doxorubicin elimination. Epistasis analysis suggested that *ELM1* functions upstream of Pdr1-mediated *PDR5* transcription. This *ELM1–PDR5* genetic connection is independent of the *SNF1* pathway. We also show that *elm1*Δ alters nucleosome structure upstream of the established Pdr1-binding sites in the *PDR5* promoter (Katzmann *et al.* 1996). However, Myc-tagged Elm1 is not detectable on the *PDR5* promoter. In summary, our studies indicate a novel link between regulation of multidrug resistance and cell cycle progression in *S. cerevisiae*, involving genes encoding key serine/threonine kinases acting during mitosis.

MATERIALS AND METHODS

Chemicals and solutions: Doxorubicin HCl (MW 579.99) solution (3.45 mm) was obtained from GensiaSicor Pharmaceuticals (Irvine, CA). FK506 (tacrolimus, Prograf, MW 822) solution (5 mg/ml = 6.08 mm) was obtained from Fujisawa (Deerfield, IL). The remaining reagents were purchased from Sigma-Aldrich (St. Louis). Sodium methanesulfonate solution used for HPLC was prepared from 15.4 m methane sulfonic acid by addition of one equivalent of sodium hydroxide and dilution to 4.0 m.

Yeast strains, genetic manipulations, agar plate drug resistance assays, and measurements of cellular respiration: Yeast cells were grown in rich (YPD) or synthetic media according to standard procedures (Sherman 1991). The genotypes of yeast strains used in this study are listed in Table 1 (Wolfger *et al.* 1997; Gao *et al.* 2004) and described previously for deletion strains derived from BY4741 (Milgrom *et al.* 2005). The null alleles introduced into *pdr1-3* were carried out by PCR-mediated allele transfer from deletion alleles of nonessential genes available from the collection of synthetic genetic arrays (Tong *et al.* 2001) or by PCR-based gene deletion using modification cassettes as previously described (Longtine *et al.* 1998). The strain with the upstream *PDR5* promoter region replaced (WCS651, Table 1) was generated by using the following primers to amplify a *TRP1* fragment from the pRS404 vector: *PDR5*-F1, 5′-CTTTTGTACGATTTTAAACAGTAAAATCGATGCATATTAAGGGAGGCCCCGGATCCCCGGGTTAATTAA-3′ (with underlined sequences being *PDR5* specific) and *PDR5*-R1, 5′-GGTAATTTGATGTTCTTTTTTTTCTTTGATTTGAACTTTTGTTCTCTCTCTGAATTCGAGCTCGTTTAAAC-3′. The WCS651 strain generated bears a deletion from −726 to −1123 (relative to the transcription start site) and was replaced with *TRP1* (1049 bp). Myc or GFP tags were introduced at the 3′-end of the *PDR1* and *PDR5* coding sequences by PCR-mediated modification (Longtine *et al.* 1998). *PDR5* mRNA

TABLE 1

***S. cerevisiae* strains used in this study**

Strain	Genotype	Source
WCS261 (YALF-A1)	*MAT***a** *ura3-52 leu2-3,112 his3-11,15 trp1-1 pdr1-3*	Wolfger *et al.* (1997)
WCS262 (YALF-I1)	*MAT***a** *ura3-52 leu2-3,112 his3-11,15 trp1-1 PDR1*	Wolfger *et al.* (1997)
WCS263 (YALF-A3)	*MAT***a** *ura3 leu2 his3 trp1-1 ade2 pdr3-2*	Wolfger *et al.* (1997)
WCS264 (YALF-O4)	*MAT***a** *ura3 leu2 his3 trp1-1 ade2 PDR3*	Wolfger *et al.* (1997)
WCS265 (FY1679-28C)	*MAT***a** *ura3-52 leu2Δ1 his3Δ200 trp1Δ63*	Wolfger *et al.* (1997)
WCS266 (FY1679-28C/*pdr3::HIS3*)	*MAT***a** *ura3-52 leu2Δ1 his3Δ200 trp1Δ63 pdr3::HIS3*	Wolfger *et al.* (1997)
WCS267 (FY1679-28C/*pdr1::TRP1 pdr3::HIS3*)	*MAT***a** *ura3-52 leu2Δ1 his3Δ200 trp1Δ63 pdr1::TRP1 pdr3::HIS3*	Wolfger *et al.* (1997)
WCS268 (FY1679-28C/*pdr1::KanMx6*)	*MAT***a** *ura3-52 leu2Δ1 his3Δ200 trp1Δ63 pdr1::Kan-Mx6*	Wolfger *et al.* (1997)
WCS345	*MAT***a** *ura3-52 leu2-3,112 his3-11,15 trp1-1 pdr1-3 elm1-300*	This study
WCS347 (YALF-C3)	*MAT*α *ura3-52 leu2-Δ1 his3-Δ200 trp1-1ade2-101och pdr1-3*	This study
WCS355	*MAT***a** *ura3-52 leu2-3,112 his3-11,15 trp1-1 pdr1-3 elm1-300* (pRS415-*ELM1*)	This study
WCS356	*MAT***a** *ura3-52 leu2-3,112 his3-11,15 trp1-1 pdr1-3 elm1-300* [pRS415]	This study
WCS489	*MAT***a** *ura3-52 leu2-3,112 his3-11,15 trp1-1 pdr1-3 nap1::LEU2*	This study
WCS490	*MAT***a** *ura3-52 leu2-3,112 his3-11,15 trp1-1 pdr1-3 gin4::LEU2*	This study
WCS491	*MAT***a** *ura3-52 leu2-3,112 his3-11,15 trp1-1 pdr1-3 cla4::KanMX*	This study
WCS492	*MAT***a** *ura3-52 leu2-3,112 his3-11,15 trp1-1 pdr1-3 elm1::LEU2*	This study
WCS496	*MAT***a** *ura3-52 leu2-3,112 his3-11,15 trp1-1 pdr1-3 mih1::KanMX*	This study
WCS497	*MAT***a** *ura3-52 leu2-3,112 his3-11,15 trp1-1 pdr1-3 swe1::TRP1*	This study
WCS501	*MAT***a** *ura3-52 leu2-3,112 his3-11,15 trp1-1 pdr1-3 pdr5::KanMX*	This study
WCS502	*MAT***a** *ura3-52 leu2-3,112 his3-11,15 trp1-1 pdr1-3 pdr5::KanMX elm1::LEU2*	This study
WCS503	*MAT***a** *ura3-52 leu2-3,112 his3-11,15 trp1-1 pdr1-3 cdc28:LEU2* (pRS316-*CDC28*)	This study
WCS504	*MAT***a** *ura3-52 leu2-3,112 his3-11,15 trp1-1 pdr1-3 cdc28:LEU2* (pRS316-*cdc28-Y19F*)	This study
WCS505	*MAT***a** *ura3-52 leu2-3,112 his3-11,15 trp1-1 pdr1-3 cdc28:LEU2* (pRS316-*cdc28-C127Y*)	This study
WCS506	*MAT***a** *ura3-52 leu2-3,112 his3-11,15 trp1-1 pdr1-3-Myc-HIS3*	Gao *et al.* (2004)
WCS507	*MAT***a** *ura3-52 leu2-3,112 his3-11,15 trp1-1 PDR1-Myc-HIS3*	Gao *et al.* (2004)
WCS530	*MAT***a** *ura3-52 leu2-3,112 his3-11,15 trp1-1 pdr1-3 PDR5-Myc*	This study
WCS531	*MAT***a** *ura3-52 leu2-3,112 his3-11,15 trp1-1 PDR1 PDR5-Myc*	This study
WCS532	*MAT***a** *ura3-52 leu2-3,112 his3-11,15 trp1-1 pdr1-3 PDR5-GFP*	This study
WCS533	*MAT***a** *ura3-52 leu2-3,112 his3-11,15 trp1-1 PDR1 PDR5-GFP*	This study
WCS534	*MAT***a** *ura3-52 leu2-3,112 his3-11,15 trp1-1 PDR1 cdc28:LEU2* (pRS316-*CDC28*)	This study
WCS535	*MAT***a** *ura3-52 leu2-3,112 his3-11,15 trp1-1 PDR1 cdc28:LEU2* (pRS316-*cdc28-Y19F*)	This study
WCS536	*MAT***a** *ura3-52 leu2-3,112 his3-11,15 trp1-1 PDR1 cdc28:LEU2* (pRS316-*cdc28-C127Y*)	This study
WCS651	*MAT***a** *ura3-52 leu2-3,112 his3-11,15 trp1-1 PDR1 pdr5 promoter*Δ *400*	This study

was induced by treatment of cells for 45 min in YPD medium containing 0.2 μg/ml (0.71 μM) cycloheximide (CYH) as described (Gao *et al.* 2004; Milgrom *et al.* 2005).

Agar plate drug resistance assays were carried out as follows. Strains were spotted (at sequential 10-fold dilutions) on plates containing either YPD or complete synthetic medium with indicated amino acids omitted. Images were taken after incubation at 30° for 3 days. Plates containing 0.2 μg/ml CYH (Figure 4E), 1.0 μg/ml CYH (Figure 1A; Figure 4, A–C; Figure 6B), or 15 μg/ml fluconazole (FLU; Figure 1A) were used in the agar plate drug resistance assay.

Cellular respiration was measured at 25° in sealed vials containing 10^7 cells as described (Souid *et al.* 2003). The cells were suspended in 1.0 ml medium, containing 6.0 mM Na_2HPO_4, 10 mM glucose, 2.0 μM Pd phosphor [Pd(II) complex of *meso*-tetra-(4-sulfonatophenyl)-tetrabenzoporphyrin], and 1.0% (w/v) fat-free bovine serum albumin. The rate of cellular respiration was determined as the negative slope of the curve of $[O_2]$ *vs.* time (in micromolars O_2/min/10^7 cells). These measurements reflected mainly mitochondrial respiration because addition of 1.0 mM NaCN completely inhibited oxygen consumption.

Ethylmethane sulfonate mutagenesis and identification of *elm1-300* mutation: The ethylmethane sulfonate (EMS) mutagenesis protocol was performed as described (Lawrence 1991; Milgrom *et al.* 2005), using a concentration of EMS (15 μl/ml of cell culture, final 15 mM) that gave 50% cell survival. Log-phase *pdr1-3* cells (~5×10^7 cells/ml of WCS261, Table 1) were treated with EMS, and 8×10^4 cells were screened for mutants that failed to grow on 1.0 μg/ml CYH by replica plating. Seven mutants showed a clear loss of CYH resistance. These were mated with the opposite mating type of the *pdr1-3* strain (WCS347, Table 1). We noted that *pdr1-3* is dominant over *PDR1* in terms of drug resistance (Wolfger *et al.* 1997). Tetrad analysis of the resulting diploid progeny indicated that two of the seven mutants (WCS343 and WCS345) harbored a single recessive mutation responsible for the loss of CYH resistance. Strain WCS345 was transformed with a YEp13-based wide-type genomic DNA library to clone the corresponding wild-type gene of the suppressor mutation. The resulting transformants were selected for restoration of CYH resistance. To exclude the possibility that recovery of CYH resistance in WCS345 was due to overexpression of genomic DNA inserted into the YEp13 vector, we subcloned the insert into a low-copy-number pRS415 plasmid (Sikorski and Hieter 1989) and repeated the test for restoration of drug resistance in WCS345. Analysis of various subclones of genomic inserts confirmed *ELM1* as the wild-type gene corresponding to the single recessive allele introduced by EMS in the WCS345 strain. The *elm1* allele responsible for loss of CYH resistance was cloned by PCR from genomic DNA of the WCS345 strain and sequenced.

Mapping *PDR5* chromatin structure by micrococcal nuclease and Northern and Western blots: The detailed mapping of the *PDR5* promoter in *pdr1-3* and *pdr1-3 elm1*Δ strains (Figure 8A) was essentially as described (Gao *et al.* 2004). The following modifications were made for mapping data presented in Figure 8B. First, *Cla*I instead of *Hin*dIII digestion was used for mapping nucleosome structures upstream known as PDREs. Second, ^{32}P-labeled probes for Southern blot analysis were generated from genomic PCR product (273 bp) of primers 5′-CGATGCATATTAAGGGAGGCC-3′ and 5′-CGCTTCCT TTGTATGATATC-3′. Preparation of total RNA and Northern blot analysis were performed as described (Shen and Green 1997; Gao *et al.* 2004). Probes for *PDR5*, *SWI5*, *PDR12*, and *ADH1* transcripts were obtained by PCR amplification from genomic DNA. Preparation of whole-cell extract by glass bead disruption was performed as described (Walker *et al.* 1997) and protein samples were subjected to SDS–polyacrylamide gel electrophoresis and immunoblotting (Harlow and Lane 1988). The mouse monoclonal antibodies against c-Myc (9E10 clone), GFP antibody, glucose-6-phosphate dehydrogenase (G6PD) antibody, and antibody α-tubulin (12G10 clone) were purchased from Santa Cruz Biotechnology (Santa Cruz, CA), Roche Diagnostics, Sigma, and the Developmental Studies Hybridoma Bank at University of Iowa, respectively. Quantification of relative mRNA and protein levels was performed using a PhosphorImager (model 425, Molecular Dynamics, Sunnyvale, CA).

Cell synchronization: Cell synchronization with nocodazole or α-factor was performed as described (Amon 2002). Yeast strains bearing the *pdr1-3* allele or a 3′ Myc-tagged *pdr1-3* allele were grown in YPD at 30° to A_{600} of ~0.3. Samples were removed for the asynchronous controls. For metaphase arrest, nocodazole (20 μg/ml) was added to the cultures. When >90% of the cells showed the characteristic arrest (equal size of budded mother–daughter cells), cells were collected by centrifugation and washed twice with 2 vol of YPD, and the pellets were resuspended in an equal volume of YPD. Samples were taken at time zero for RNA preparation or incubated with 50 μM doxorubicin for 15 min for measurement of cellular doxorubicin. Microscopic examination of cells harvested throughout the experiments confirmed that cells sampled at time zero were arrested at mitosis and revealed approximation of various stages during a cell cycle. The synchronized cultures continued to grow at 30°, and samples were taken at 15-min intervals for preparations of RNA and measurement of intracellular doxorubicin after incubation with 50 μM doxorubicin for 15 min. There was no apparent cell cycle progression during the 15-min incubation with doxorubicin, consistent with the antiproliferative effect of the drug in mammalian cells (Harisi *et al.* 2005) and yeast (our observation).

Growth of cultures for G_1 arrest by α-factor was essentially the same as metaphase arrest by nocodazole. The concentration of α-factor used for synchronization was 3 μg/ml, and the characteristic schmoo phenotype, indicating G_1 arrest, was confirmed microscopically.

Chromatin immunoprecipitation: The condition for formaldehyde-based *in vivo* crosslinking and chromatin immunoprecipitation (ChIP) was as described (Gao *et al.* 2004; Milgrom *et al.* 2005). The immunoprecipitations were performed using anti-Myc antibody. The following sets of primers were used for the PCR analysis: *PDR5* (UAS), 5′-TCGTGATCACGATTCAG CACC-3′ and 5′-GGAGAGGCCTTGTTTGTATTGC-3′; *PDR5* (middle of the *co*ding *s*equences, CDS), 5′-GAAAGCTCTGAA GAGGAATCC-3′ and 5′-CCCTTTCGGCCAAACAATCCA-3′; *PDR12* (promoter), 5′-CACATTTTCTCGACGGTTC-3′ and 5′-GTAACTGGGAAAACAGAG-3′.

Cellular doxorubicin determination: For cellular doxorubicin efflux, log-phase cells were incubated at 30° in YPD plus 50 μM doxorubicin for 60 min. The cells were collected by centrifugation, resuspended in drug-free YPD (prewarmed to 30°), and incubated at 30° for various periods of time. Aliquots of the cell suspension were then spun at specific time points. The pellets were suspended in 250 μl of 10% perchloric acid/2.0 M Na methanesulfonate. Equal volumes of glass beads were added, and the suspensions were vigorously vortexed for 3.0 min. The acid-soluble supernatants were separated on HPLC and analyzed as described below.

For cellular doxorubicin accumulation, log-phase cells were incubated in YPD media plus 50 μM doxorubicin at 30° for various periods of time. The cells were collected by centrifugation and the pellets were immediately chilled on ice. The cold pellets were washed twice with ice-cold double-distilled H_2O containing 20 μM FK506, a known inhibitor of the ABC transporters (Egner *et al.* 1998). The washed pellets were then

suspended in 250 μl of 10% perchloric acid/2.0 M sodium methanesulfonate. Equal volumes of glass beads were added, and the suspensions were vigorously vortexed as described above.

Doxorubicin peaks were detected by fluorescence (excitation, 480 nm; emission, 560 nm) as described (Fogli *et al.* 1999). The analysis was performed on a Beckman HPLC system. The solvent used was 60% of 50 mM NaH_2PO_4 (pH ~3.5) and 40% of acetonitrile. The column (4.6 × 250-mm Beckman ultrasphere IP) was operated isocratically at 0.5 ml/min. Standards (10 μM doxorubicin in 10% perchloric acid/2.0 M sodium methanesulfonate) were included with each analytical run. Peaks were identified (doxorubicin retention time, ~13.8 min) and quantitated using doxorubicin standards, with the minimal quantifiable level of doxorubicin (~10 pmol) giving a signal: noise ratio of 3:1. Cellular doxorubicin was expressed in picomoles/10^7 cells on the basis of microscopic enumeration. Standard deviations were derived from at least three sets of experiments. Treating of *PDR1* and *pdr1-3* cells with 50 μM doxorubicin for 15–120 min did not induce *PDR5* expression (our observation). Statistical significance between values in different strains was determined by paired Student's *t*-test analyses. A value of $P < 0.05$ was considered significant.

RESULTS

Characterization of Pdr1-mediated multidrug resistance—a critical role for *PDR5* in cellular doxorubicin efflux: The transcription of several ABC transporter genes (including *PDR5*) is upregulated in the *pdr1-3* strain (WCS261), which is resistant to CYH and the antifungal drug FLU. Introducing *pdr5*Δ into the *pdr1-3* strain resulted in loss of multidrug resistance, confirming *PDR5* as the major transporter target of Pdr1 (Figure 1A). The impact of CYH treatment (0.2 μg/ml) in our study on the stability of *PDR5* mRNA was investigated in the *rpb1-1* strain, which carried a temperature-sensitive mutation in the largest subunit of RNA polymerase II. After thermal inactivation of the *rpb1-1* allele, $t_{1/2}$ for *PDR5* mRNA was ~20 min in either the presence or the absence of the CYH condition (our observation), consistent with the estimation by microarray analysis (Holstege *et al.* 1998). Thus, our Northern blot analyses of *PDR5* reflect transcription levels rather than stability of mRNA.

Compared to wild-type *PDR1*, an ~10-fold increase in *PDR5* mRNA was found in the *pdr1-3* strain (DeRisi *et al.* 2000; Gao *et al.* 2004), and further induction occurred with CYH treatment (Gao *et al.* 2004). To compare the level of Pdr5 protein in *PDR1 vs. pdr1-3*, we introduced sequences encoding a 13xMyc tag or GFP tag at the 3′-end of the *PDR5* coding sequence. The tagged version of *PDR5* was functional, indicated by normal resistance to several drugs (not shown). An ~10-fold increase in Pdr5 protein was observed in *pdr1-3* relative to *PDR1* (Figure 1B; note the 10-fold lower G6PD loading control in the *pdr1-3* lane). Pdr5 protein was inducible by CYH in both *pdr1-3* (Figure 1C) and *PDR1* strains (not shown). The comparable increases in both *PDR5* mRNA and Pdr5 level in the *pdr1-3* strain relative to the *PDR1* strain confirmed transcriptional regulation as a crucial step for

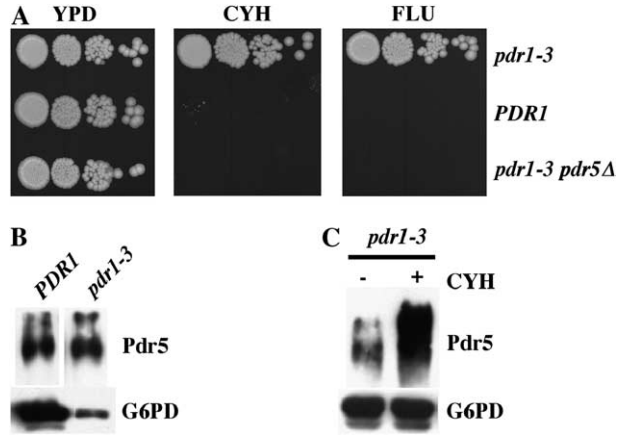

Figure 1.—Role of *PDR5* in multidrug resistance of the *pdr1-3* strain. (A) Agar plate drug resistance assay showing the drug susceptibility of *pdr1-3*, *PDR1*, and *pdr1-3 pdr5*Δ. Cells (10^7 cells and sequential 10-fold dilutions of each strain) were spotted onto YPD plates with and without CYH (1.0 μg/ml) or FLU (15 μg/ml). Images were taken after 30° incubation for 3 days. (B) Western blot analysis of Pdr5 (Myc-tagged) in the *PDR1* (40 μg of the whole-cell lysate) and *pdr1-3* (4 μg of the whole-cell lysate) strains. G6PD served as a loading control. (C) Western blot analysis of Pdr5 (GFP tagged) in the *pdr1-3* strain in the presence and absence of CYH (0.2 μg/ml for 45 min). Forty micrograms of the whole-cell lysate were loaded in each lane.

PDR5-mediated drug resistance in *S. cerevisiae* (Moye-Rowley 2003).

Doxorubicin is a known substrate of many ABC transporters (Eytan 2005) and deletion of *PDR5* leads to hypersensitivity to doxorubicin and many other drugs (Rogers *et al.* 2001; Golin *et al.* 2003). Transport activities for doxorubicin were determined by analytically detecting the fluorescence of the drug in acid soluble supernatants extracted from cells and separated by HPLC (Figure 2A). In the presence of FK506, a known inhibitor of ABC transporters, including Pdr5 (Egner *et al.* 1998), cells accumulated approximately ninefold more doxorubicin than in its absence (compare doxorubicin peaks in Figure 2, A and B; note the different cell number count in each condition). FK506 appears to prevent the interactions between Pdr5 and its substrates directly. Changes of a single residue of the Pdr5 transmembrane domain 10 (for example, S1360F, T1364F, and T1364A) alter both substrate specificity and susceptibility to FK506 (Egner *et al.* 1998, 2000).

A time-course study was used to compare the relative accumulation of doxorubicin by the *PDR1* and *pdr1-3* strains. During the first 15 min of incubation with the drug, doxorubicin content was similar in the *PDR1* and *pdr1-3* cells (Figure 2C). Thereafter, the difference between the two strains increased, with accumulation being higher in *PDR1*. Cellular doxorubicin reached a plateau after ~50 min, about twice as high in *PDR1* as in *pdr1-3* (Figure 2C). On the basis of this study, we preincubated the cells with 50 μM doxorubicin for 60 min

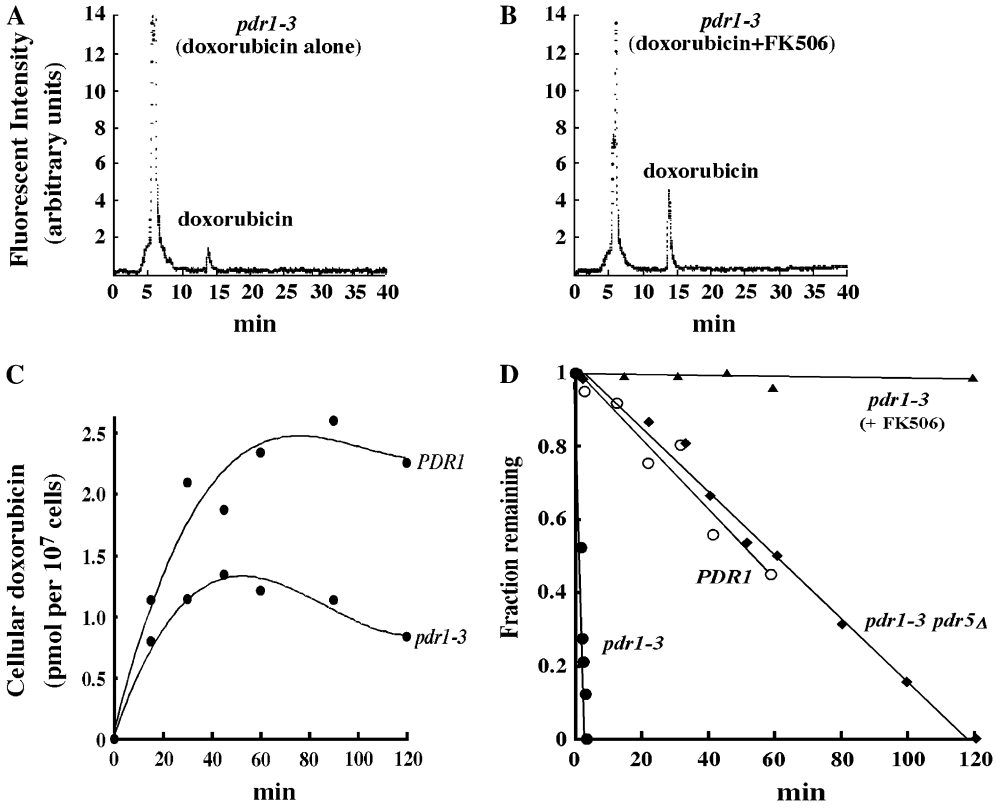

FIGURE 2.—Kinetics of doxorubicin accumulation in *PDR1* and *pdr1-3* strains. Representative HPLC chromatograms for the *pdr1-3* strain treated at 30° with 50 μM doxorubicin alone (A) or 50 μM doxorubicin plus 20 μM FK506 (B). Doxorubicin peaks had a retention time of ~13.8 min. The volume (60 μl) injected into HPLC for doxorubicin alone corresponded to $\sim 8.9 \times 10^7$ cells and for doxorubicin plus FK506 to $\sim 2.0 \times 10^7$ cells. The first peak corresponded to the solvents. (C) Doxorubicin accumulation as a function of time in *PDR1* and *pdr1-3* strains. Cellular doxorubicin content was expressed as picomoles/10^7 cells. The cells were incubated with 50 μM doxorubicin at 30° for the indicated time. (D) Doxorubicin efflux rates in the *pdr1-3* (±FK506), *PDR1* (−FK506), and *pdr1-3 pdr5*Δ (−FK506) strains. The cells were incubated with 50 μM doxorubicin at 30° for 60 min. The cells were then washed and incubated in drug-free media for the indicated time periods. The fraction of doxorubicin retained by the cells was plotted against incubation time in drug-free medium. The efflux rate constants were determined as the negative slopes of the best-fit lines and summarized in Table 2.

to visualize the rates of drug elimination (Figure 2D), while drug accumulation was measured by incubating cells with 50 μM doxorubicin for 15 min (Figure 3B). The rate of drug efflux was determined by measuring the fraction of the drug remaining in the cells after incubation in drug-free medium. The resulting best-fit lines (Figure 2D) gave r^2 values for *pdr1-3* of 0.975 and for *pdr1-3 pdr5*Δ of 0.990, which is consistent with a kinetic study of P-glycoprotein (AMBUDKAR *et al.* 1997) and a process ensuring complete elimination of the drug. The zero-order rate constant (k), calculated as the negative slope of the best-fit straight line, was $\sim 48 \times 10^{-4}$/sec for the *pdr1-3* and $< 0.1 \times 10^{-4}$/sec in the presence of 20 μM FK506. Cellular doxorubicin elimination was therefore negligible in the presence of the inhibitor FK506. The k values for *pdr1-3 pdr5*Δ and *PDR1* were comparable, $\sim 1.4 \times 10^{-4}$/sec and $\sim 1.5 \times 10^{-4}$/sec, respectively, which were at least 30-fold lower than that for the *pdr1-3* strain (Table 2). Significantly, the *pdr1-3 pdr5*Δ strain exhibited a drug efflux rate similar to that in *PDR1* (Figure 2D), underscoring the pivotal role of Pdr5 in Pdr1-regulated cellular detoxification. The nonlinear relationship between the increased doxorubicin efflux (~30-fold relative to *PDR1*, Table 2) and the upregulation of *PDR5* expression (~10-fold relative to *PDR1*, Figure 1) may reflect the collective activity of several transporters known to be overexpressed in the *pdr1-3* strain (DERISI *et al.* 2000). Other factors might include altered patterns of post-translational modifications on Pdr5, such as ubiquitination (EGNER and KUCHLER 1996), phosphorylation (CONSEIL *et al.* 2001), and glycosylation (JAKOB *et al.* 2001) in the *pdr1-3* strain, which in turn contributed to the effectiveness of the drug transporter functions.

Cyclic levels of *PDR5* mRNA and cellular doxorubicin during cell cycle progression: We next analyzed *PDR5* mRNA fluctuation during the cell cycle. We synchronized *pdr1-3* cells with nocodazole and monitored *PDR5* transcript levels and cellular doxorubicin concentration during cell cycle progression (Figure 3). *PDR5* transcripts varied considerably during the cell cycle and peaked concurrently with *SWI5* mRNA accumulation, a known marker of mitosis (Figure 3A). *PDR5* mRNA was approximately fourfold higher at the M phase than at the G_1 phase (Figure 3B, diamonds and solid line). Cellular doxorubicin, on the other hand, was about fourfold lower at the M phase than at the G_1 phase (Figure 3B, circles and dotted line). Similar phase-related behavior was seen with *PDR5* mRNA and cellular doxorubicin during cell cycle progression in synchronized *PDR1* cells (not shown). These results indicated that *PDR5* mRNA accumulation was cell cycle controlled. Moreover, the inverse relationship between *PDR5* mRNA and cellular doxorubicin suggested that *PDR5* expression

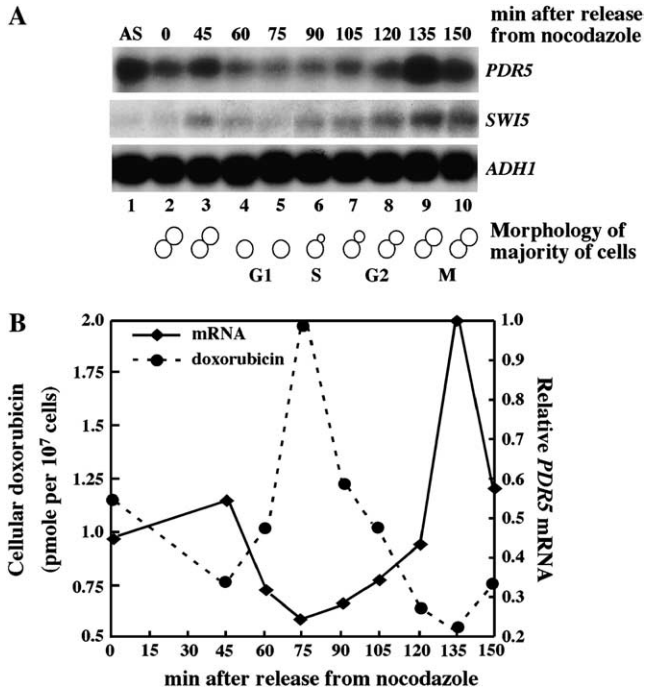

FIGURE 3.—*PDR5* mRNA and doxorubicin efflux both peak at mitosis. (A) Northern blot analysis of *PDR5* showing mRNA levels during the cell cycle. The blot was also probed for *SWI5* and *ADH1* mRNA. The *pdr1-3* strain was synchronized in media containing 20 μg/ml nocodazole and then released. Total RNA was harvested at the indicated time postrelease. Morphologically, the period between 45 min and 135 min after nocodazole release corresponded to a complete cell cycle. AS, asynchronous. (B) Levels of doxorubicin during the cell cycle. In an experiment parallel to A, cells were harvested at the indicated time and immediately placed in medium containing 50 μM doxorubicin for 15 min. Dashed lines indicate cellular doxorubicin; solid lines indicate relative *PDR5* mRNA. Cellular doxorubicin content was expressed as picomoles/10^7 cells. The level of mRNA at 135 min is denoted as 1.0.

might alter cellular susceptibility to drugs during the cell cycle, with the greatest susceptibility during G_1 phase and the least susceptibility during M phase. The possibility that regulatory mechanisms might modulate *PDR5* expression during cell cycle progression prompted us to search for genes affecting this aspect of *PDR5*-mediated drug resistance.

Mutation of *ELM1* suppresses *PDR5* transcription and drug resistance: We then performed a genetic screen for extragenic suppressors of CYH resistance in the *pdr1-3* haploid strain (WCS 261). We searched for factors that regulate drug resistance mediated by *PDR5*. Screening of ~80,000 EMS-treated colonies gave seven candidates showing loss of resistance. Two of the seven candidate haploid *pdr1-3* strains harbored additional single recessive mutations as indicated by CYH resistance of the homozygous diploid *pdr1-3* strains resulting from mating candidate suppressor strains to an isogenic *pdr1-3* strain of the opposite mating type (WCS347) and from segregation of 2:2 resistant and sensitive spores derived

TABLE 2

Doxorubicin efflux rates in yeast mutant strains

Strains	Efflux rate	Relative efflux rate
PDR1	1.5×10^{-4}/sec	1
pdr1-3	48×10^{-4}/sec	32
*pdr1-3 pdr5*Δ	1.4×10^{-4}/sec	0.93
*pdr1-3 nap1*Δ	1.2×10^{-4}/sec	0.8
*pdr1-3 gin4*Δ	$\sim 0.4 \times 10^{-4}$/sec	0.27
*pdr1-3 cla4*Δ	$< 0.2 \times 10^{-4}$/sec	<0.13
*pdr1-3 elm1*Δ	$< 0.2 \times 10^{-4}$/sec	<0.13
pdr1-3 cdc28-C127Y	$< 0.2 \times 10^{-4}$/sec	<0.13
pdr1-3 cdc28-Y19F	46×10^{-4}/sec	31

The efflux rates of indicated strains were the negative slopes derived from time-course experiments as described in Figure 2D in the absence of FK506. Relative efflux rates were normalized to the *PDR1* strain.

from each tetrad. In one of the two mutants, WCS345, the corresponding wild-type gene of the extragenic suppressor allele was cloned by complementation from a high-copy genomic library. Sequencing the clones identified a 6-kb fragment of chromosome XI, carrying the two complete genes *ELM1* and *CSE4*. Microscopic examination of the WCS345 strain demonstrated elongated bud morphology, indicating a G_2 delay (Figure 4A, left, *pdr1-3 elm1-300*), a phenotype reminiscent of *elm1* mutations (KOEHLER and MYERS 1997). A low-copy plasmid pRS415 (SIKORSKI and HIETER 1989) harboring *ELM1* (p*ELM1*) restored CYH resistance (Figure 4A, bottom left) and rescued the elongated bud morphology of *pdr1-3 elm-300* (not shown). The mutant *elm1* allele from the WCS345 strain was cloned and sequenced. The allele harbored a C-to-T mutation in the coding region, converting glutamine 301 (CAG) to a stop codon (TAG) and was therefore termed *elm1-300* (Figure 4A). This truncation deleted part of the kinase domain of Elm1, which spans amino acid residues 88–406 (KOEHLER and MYERS 1997; Figure 4A). The Elm1 kinase domain contains two stretches of amino acid residues that match the consensus sequence of Ser/Thr kinases (BLACKETER *et al.* 1993; KOEHLER and MYERS 1997). The *elm1-300* mutation eliminated completely the second consensus sequence, GTPAFIAPE (amino acid residues 309–317; Figure 4A).

The level of *PDR5* mRNA in *pdr1-3 elm-300* was significantly lower than in *pdr1-3*, and CYH failed to fully induce *PDR5* transcription (Figure 4B), indicating that both noninduced (constitutive) and drug-induced transcriptions of *PDR5* were reduced in *pdr1-3 elm-300*. These transcriptional defects were rescued by introducing wild-type *ELM1* on a low-copy plasmid, p*ELM1*, into the *pdr1-3 elm-300* strain (Figure 4B). Therefore, *ELM1* was required for proper constitutive and drug-induced *PDR5* transcription.

To further test the effect of *elm1*, we introduced the *elm1*Δ allele into *pdr1-3* (Figure 4C) and *PDR1* (Figure 4D)

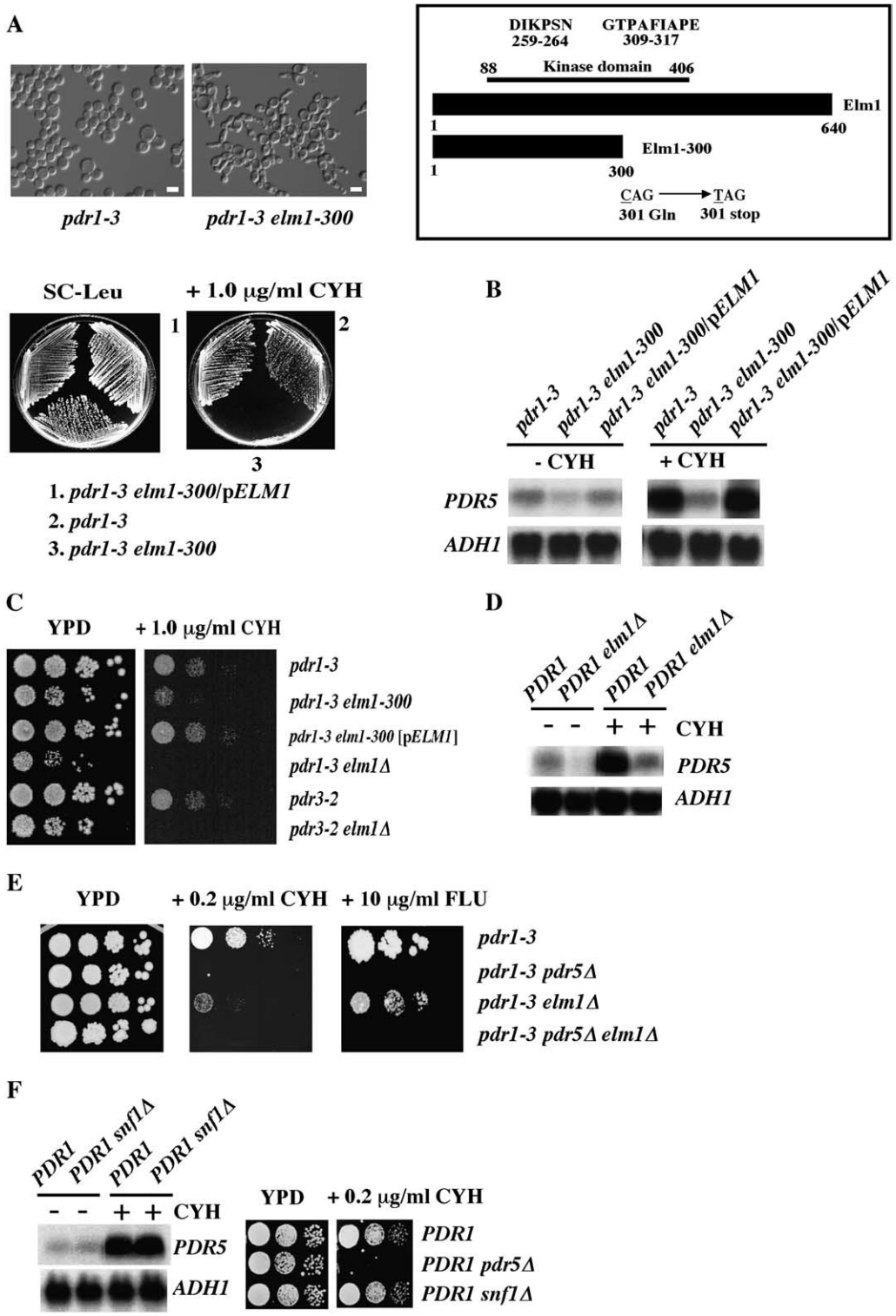

FIGURE 4.—Mutations in *ELM1* suppressed CYH resistance mediated by the *pdr1* and *pdr3* mutations in a *SNF1*-independent manner. (A, top left) Elongated morphology (an indication of G_2 delay) of the *pdr1-3 elm1-300* strain. Bar, 5 μm. (Bottom left) Loss of CYH resistance in *pdr1-3 elm1-300*. The *pdr1-3 elm1-300* strain was transformed with a single-copy pRS415 plasmid derivative containing wild-type *ELM1* (p*ELM1*), which complemented the *elm1-300* mutation. The pRS415 was a centromere-based plasmid marked with *LEU2*. Images were taken after growth on complete synthetic medium minus leucine with and without 1.0 μg/ml CYH at 30° for 3 days. (Top right) The kinase domain of Elm1 and truncation of Elm1-300. (B) Northern blot analysis of *PDR5* mRNA in *pdr1-3*, *pdr1-3 elm1-300*, and *pdr1-3 elm1-300* (p*ELM1*) strains in the presence and absence of CYH (0.2 μg/ml for 45 min). *ADH1* served as a loading control. The strains were grown in complete synthetic medium minus leucine for plasmid retention. (C) Agar plate drug resistance assays of *pdr1-3* and *pdr3-2* strains harboring either *elm1-300* or *elm1*Δ mutation on YPD with or without 1.0 μg/ml CYH. Cells harboring plasmids were grown in synthetic selective medium before spotting. Images were taken after 30° incubation for 3 days. (D) Northern blot analysis of *PDR5* mRNA in *PDR1* and *PDR1 elm1*Δ strains in the presence and absence of CYH (0.2 μg/ml for 45 min). (E) Agar plate drug resistance assays of *pdr1-3*, *pdr1-3 pdr5*Δ, *pdr1-3 elm1*Δ, and *pdr1-3 pdr5*Δ *elm1*Δ strains on YPD with or without 0.2 μg/ml CYH, 10 μg/ml fluconazole (performed as described in C). (F, left) Northern blot analysis of *PDR5* mRNA in *PDR1* and *PDR1 snf1*Δ strains in the absence and presence of CYH induction. (Right) Agar plate drug resistance compared to CYH resistance of *PDR1*, *PDR1 pdr5*Δ, and *PDR1 snf1*Δ strains on YPD medium with and without 0.2 μg/ml CYH; the three strains are in a BY4741 background.

strains. The *pdr1-3 elm1*Δ strain was more sensitive to CYH than *pdr1-3 elm1-300* was (Figure 4C), suggesting a residual function of *ELM1* in the *elm1-300* allele. Loss of CYH resistance was also observed when the *elm1*Δ allele was introduced to another drug resistant strain, *pdr3-2*, that overexpressed *PDR5* (DELAVEAU *et al.* 1994) (Figure 4C). These data indicated that the observed *elm1*Δ effects were not *pdr1-3* allele specific. Compared

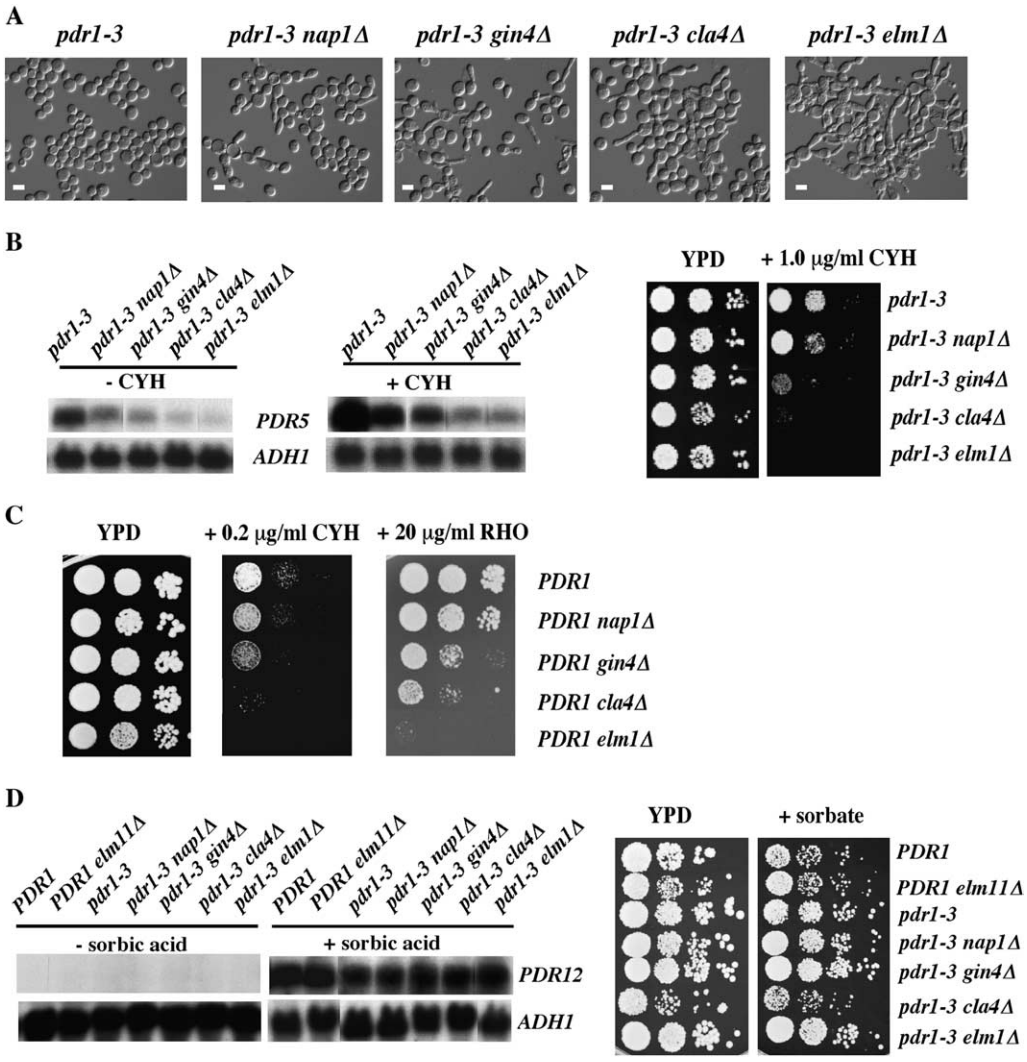

FIGURE 5.—Mutations causing a defective mitotic progression gave elongated bud morphology, loss of drug resistance, and reduced *PDR5* transcription. (A) Elongated bud morphology of the strains bearing individual null mutations of *NAP1*, *GIN4*, *CLA4*, and *ELM1*. Bar, 5 μm. (B, left) Northern blots of *PDR5* mRNA in *pdr1-3* and the strains bearing the indicated null mutations. *ADH1* served as a loading control. *PDR5* transcription was induced by 0.2 μg/ml CYH for 45 min. (Right) Agar plate drug resistance assays (performed as described in Figure 4C) show loss of CYH resistance as a result of the indicated null mutations. (C) Agar plate drug resistance assays (performed as described in Figure 4C) show loss of CYH and RHO (rhodamine) resistance as a result of the indicated null mutations in a *PDR1* strain. (D, left) Northern blots of *PDR12* mRNA in *PDR1*, *pdr1-3*, and the strains derived from *pdr1-3* bearing the indicated null mutations. *PDR12* transcription was induced by 1.0 mM sorbic acid for 45 min. (Right) Agar plate weak acid resistance assays of indicated strains grown in the absence or presence of 9 mM sorbate.

with the *PDR1* wild-type strain, the presence of the *elm1*Δ drastically reduced *PDR5* mRNA under both noninduced and induced conditions (Figure 4D). We therefore conclude that *ELM1* is required for Pdr1/Pdr3-regulated CYH resistance, which is mediated, at least partially, by *PDR5*. Epistasis analysis revealed that both *pdr1-3 pdr5*Δ *elm1*Δ and *pdr1-3 pdr5*Δ strains failed to grow in the presence of 0.2 μg/ml CYH or 10 μg/ml fluconazole whereas *pdr-1-3 elm1*Δ could survive under the same conditions (Figure 4E). These results provided genetic evidence that *ELM1* functions upstream of *PDR5* in regulation of CYH resistance.

Elm1 is an upstream activator of Snf1 kinase (HONG *et al.* 2003; SUTHERLAND *et al.* 2003). Elm1 also regulates mitotic entrance, septin formation, and cytokinesis (GARRETT 1997; KOEHLER and MYERS 1997; BOUQUIN *et al.* 2000). To test the possibility that Elm1 affects *PDR5* transcription via the Snf1-mediated pathway, *PDR5* transcription (Figure 4F, left) and CYH resistance (Figure 4F, right) were analyzed in pairwise isogenic wild-type and *snf1*Δ strains. Deletion of *SNF1* had no effect on either *PDR5* transcription or CYH resistance. These data indicate that *ELM1* regulates *PDR5* transcription via a pathway(s) independent of *SNF1*.

Mutation of genes required for mitotic progression represses *PDR5* transcription: In *S. cerevisiae*, entry into mitosis is mediated by activating CDK. As described in the Introduction, additional serine/threonine kinases (*e.g.*, *ELM1*, *GIN4*, and *CLA4*) are also involved in regulating the transition from G_2 to mitosis. We next investigated the effects on *PDR5*-mediated drug resistance by other genes that are functionally related to *ELM1* and required for proper mitotic progression. In addition to *elm1*Δ, we introduced individual null alleles of *nap1*Δ, *gin4*Δ, and *cla4*Δ into the haploid *pdr1-3* strain and analyzed their effects on cell morphology, CYH resistance, *PDR5* mRNA accumulation (Figure 5), and cellular doxorubicin efflux (Table 2). The *nap1*Δ, *gin4*Δ,

TABLE 3

Minimal inhibitory concentrations of drugs in the yeast mutant strains

Strains	CYH (μg/ml)	CHL (mg/ml)	RHO (μg/ml)
PDR1	<0.2	5	10
*pdr1-3 pdr5*Δ	<0.2	3	<2.5
pdr1-3	>1.0	7.5	>20
*pdr1-3 elm1*Δ	<0.2	<2	<2.5
*pdr1-3 cla4*Δ	0.2	2	<2.5
*pdr1-3 gin4*Δ	0.4	5	>20
*pdr1-3 nap1*Δ	0.8	5	>20

Agar plate drug resistance assays were performed with various concentrations of cycloheximide (0.2, 0.4, 0.6, 0.8, and 1.0 μg/ml), chloramphenicol (1, 2, 3, 5, 6, and 7.5 mg/ml), and rhodamine (2.5, 5.0, 7.5, 8, 10, 15, and 20 μg/ml). The *PDR5* gene has been shown to be involved in the regulation of resistance to these three drugs (Rogers *et al.* 2001). Each experiment was repeated at least twice. CHL, chloramphenicol; RHO, rhodamine.

*cla4*Δ, and *elm1*Δ alleles resulted in various degrees of elongated bud morphology (Figure 5A), decreased *PDR5* transcription (Figure 5B, left), loss of CYH resistance (Figure 5B right), and reduced doxorubicin efflux rates (Table 2), with the general order of effect on drug resistance being *elm1* > *cla4* > *gin4* > *nap1* in both the *pdr1-3* strain (Figure 5B) and the *PDR1* strain (Figure 5C). Consistent patterns of reduced growth at lower drug concentrations were also observed; the minimal inhibitory concentrations for three drugs are listed in Table 3. The *pdr1-3 elm1*Δ strain exhibited the most pronounced effects on elongated morphology, *PDR5* transcription, and drug resistance. The *pdr1-3 nap1*Δ strain exhibited relatively minor morphological changes, moderately decreased *PDR5* transcription, and slightly reduced drug resistance. It is worth noting that there was no detectable doxorubicin efflux in the *pdr1-3 elm1*Δ and *pdr1-3 cla4*Δ strains (Table 2), which is virtually identical to that observed in the presence of the inhibitor FK506 (Figure 2D). This suggests that other drug transporter genes in addition to *PDR5* are negatively affected by *elm1*Δ and *cla4*Δ, consistent with previous reports (Spellman *et al.* 1998). Significantly, however, *elm1*Δ, *cla4*Δ, *gin4*Δ, and *nap1*Δ did not affect sorbic-acid-induced *PDR12* mRNA (Figure 5D, left) or growth in the presence of sorbate (Figure 5D, right). *PDR12* encodes a weak acid anion transporter, whose transcription is independent of Pdr1 and Pdr3 (Piper *et al.* 1998; Kren *et al.* 2003). These results indicate a gene-specific transcriptional defect in these mutant strains.

Cdc28 is a master regulator of cell division in *S. cerevisiae* that controls mitotic entrance (Mendenhall and Hodge 1998). We hypothesized that a *cdc28* mutation impairing mitotic progression would suppress the multidrug resistance of *pdr1-3* in a manner comparable to that of *elm1*Δ. The *cdc28-C127Y* allele was previously shown to cause elongated bud morphology (Edgington *et al.* 1999). In contrast, the *cdc28-Y19F* allele (McMillan *et al.* 1999) is insensitive to Swe1-kinase-imposed inhibition of mitotic entrance and exhibits normal morphogenesis. We introduced these two mutant alleles into the *pdr1-3* strain and investigated their effects on *PDR5* mRNA levels and CYH resistance. As anticipated, *pdr1-3 cdc28-C127Y* exhibited reduced *PDR5* mRNA (Figure 6C), loss of CYH resistance (Figure 6B), and elongated bud morphology (Figure 6A). Like the *pdr1-3 elm1*Δ strain, doxorubicin efflux in the *pdr1-3 cdc28-C127Y* strain was negligible (Table 2). In contrast, the *pdr1-3 cdc28-Y19F* strain behaved in a manner comparable to the *pdr1-3* strain (Table 2; the difference in the efflux rate between the two strains was within the standard error). Reduced CYH resistance due to the presence of the *cdc28-C127Y*, but not *cdc28-Y19F*, allele was also observed in the *PDR1* strain (Figure 6D), indicating that the effect is not *pdr1-3* allele specific. We further analyzed the effects of Swe1 (Cdc28 kinase) and Mih1 (Cdc28 phosphatase) on *PDR5* transcription. The *swe1*Δ strain can enter mitosis like wild-type cells, whereas the *mih*Δ strain exhibits a mitotic delay (Sia *et al.* 1996). Relative to *pdr1-3* and *pdr1-3 swe1*Δ, the level of *PDR5* mRNA in *pdr1-3 mih1*Δ was significantly reduced (Figure 6E). As both *mih*Δ and *cdc28-C127Y* mutants were defective in mitotic entrance and exhibited marked reduction of *PDR5* transcription, these data reinforce the significance of *PDR5* transcription peaking during normal mitosis (Figure 2). Therefore, mitotic progression is required for optimal *PDR5* expression and development of drug resistance.

We then examined the possibility that other non-cell-cycle-related changes in these mutants (for instance, general sickness) might account for the total loss of doxorubicin efflux (Table 2). For example, it was reported that loss of signaling between nuclei and mitochondria reduces the level of *PDR5* expression and drug resistance in *rho*^{0} cells (Hallstrom and Moye-Rowley 2000). We therefore measured the rates of cellular mitochondrial oxygen consumption (cellular respiration) in these mutant strains (strains shown in Figure 5 and Figure 6). The respiration was virtually identical, 4.6 ± 0.8 μM O_2/min/10^7 cells, in all mutants studied. These results rule out that alteration of mitochondrial functions in these mutants contributes to the observed defects in *PDR5* transcription and to related loss of drug resistance. Moreover, *snf1*Δ, which exhibits a growth defect on a nonfermentable (respiratory) carbon source, did not affect *PDR5* transcription and CYH resistance (Figure 4F). Together, these data support the possibility that Elm1 and related serine/threonine kinases affect *PDR5* transcription and drug resistance by a cell-cycle-derived mechanism.

Recruitment of Pdr1 to the *PDR5* UAS is cell cycle independent: We next explored the molecular events

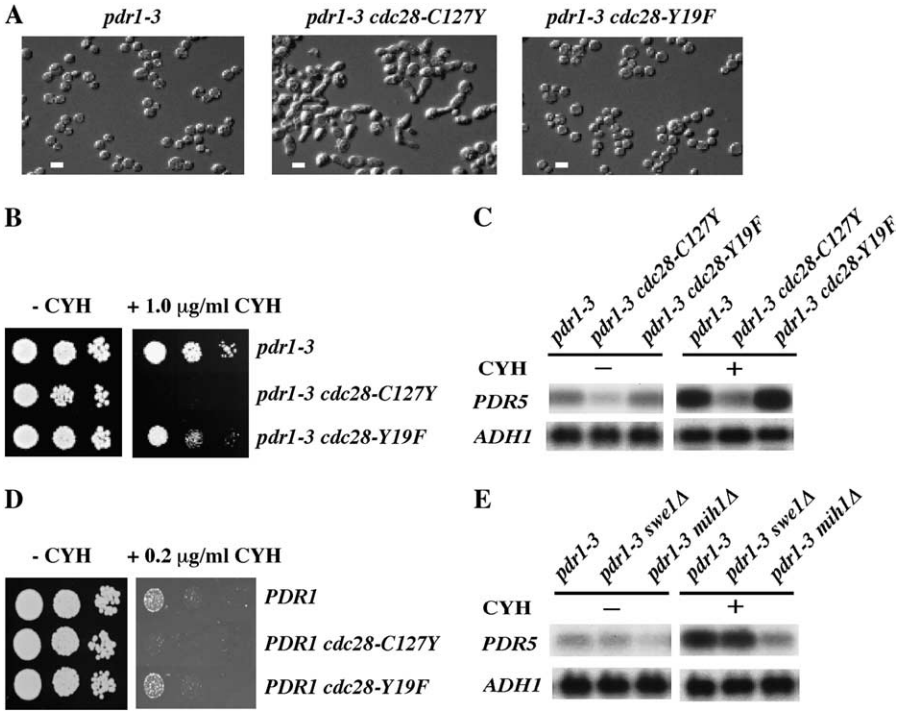

FIGURE 6.—*Cdc28-C127Y* mutation gave elongated bud morphology, loss of CYH resistance, and reduced *PDR5* transcription. (A) Elongated morphology was exhibited by the *pdr1-3 cdc28-C127Y* strain but not by the *pdr1-3* and *pdr1-3 cdc28-Y19F* strains. Bar, 5 μm. (B) Agar plate drug resistance (performed as described in Figure 4C, except that complete synthetic media minus uracil plates were used for plasmid retention) showed loss of CYH resistance in *pdr1-3 cdc28-C127Y.* (C) Northern blots of *PDR5* mRNA in the three strains showed downregulation of *PDR5* transcription in *pdr1-3 cdc28-C127Y,* but not in *pdr1-3 cdc28-Y19F. PDR5* transcription was induced by 0.2 μg/ml CYH for 45 min. (D) Agar plate drug resistance (performed as described in Figure 4C, except that complete synthetic media minus uracil plates were used for plasmid retention) showed loss of CYH resistance in *PDR1 cdc28-C127Y.* (E) Downregulation of *PDR5* transcription occurred in the *pdr1-3 mih1*Δ strain but not in the *pdr1-3 swe1*Δ strain. The CYH treatments were at 0.2 μg/ml for 45 min.

required for *PDR5* transcriptional upregulation during mitosis. We investigated whether the level of the Pdr1-3 activator and its binding to the *PDR5* promoter varied during the cell cycle. We monitored the level of Pdr1-3 during cell cycle progression by integrating a Myc-epitope tag at the 3′-end of the *pdr1-3* open reading frame (ORF). The induction of *PDR5* in this strain was identical to the nontagged parental strain (GAO *et al.* 2004). Myc-tagged Pdr1-3 was then analyzed during the cell cycle (Figure 7A). Western blot analysis of nocodazole synchronized cells showed constant Pdr1-3 levels during cell cycle progression (Figure 7A). Therefore, the fluctuating *PDR5* mRNA levels in the cell cycle (Figure 3) were not due to fluctuating Pdr1-3 levels.

We then investigated how much the Pdr1-3 activator associates with the *PDR5* promoter. A ChIP assay was used to analyze the recruitment of Myc-tagged Pdr1-3 to the *PDR5* promoter. As *PDR5* transcription is sensitive to cell cycle progression, it is possible that different synchronization protocols might interfere with activator recruitment (SHEDDEN and COOPER 2002). To test this possibility, we conducted parallel ChIP assays from cells synchronized by nocodazole or α-factor treatment and then released. The two treatments gave the same result. Successful synchronization and release at various time points thereafter by either nocodazole (Figure 7A) or α-factor (Figure 7B) were validated by microscopic examination of distinct morphologies throughout the experiments (not shown). Pdr1-3 was recruited specifically to the promoter region of *PDR5*, and no detectable Pdr1-3 was recruited to the *PDR5* CDSs (coding sequences, Figure 7B, synchronized by α-factor). Pdr1-3 recruitment to the *PDR5* promoter was constitutive and independent of the cell cycle. In fact, there was no difference in the amount of Pdr1-3 activator bound to the *PDR5* promoter as the cell cycle progressed (Figure 7B). We also performed ChIP analysis on the recruitment of wild-type Myc-tagged Pdr1 activator to the *PDR5* promoter and the results were virtually identical to the Pdr1-3 recruitment data presented in Figure 7B (data not shown). Therefore, the recruitment of Pdr1 and Pdr1-3 activators to the *PDR5* promoter was not responsible for the fluctuating levels of *PDR5* mRNA in the cell cycle.

We then analyzed Pdr1 and Pdr1-3 recruitment to the *PDR5* promoter in the presence of an *elm1*Δ allele in both *PDR1* and *pdr1-3* strains (Figure 7C). In the *elm1*Δ strains, in which the recruitment of Pdr1-3 onto the *PDR5* promoter was slightly higher than that of Pdr1 (Figure 7C), the results are virtually indistinguishable from our previous observation of Pdr1-3/Pdr1 recruitment in the presence of wild-type *ELM1* (GAO *et al.* 2004). We conclude, therefore, that the recruitment of Pdr1 is not a rate-limiting step accounting for decreased *PDR5* transcription in the *elm1*Δ strains. Collectively, the data presented in Figure 7 indicate that cell-cycle-dependent *PDR5* transcription is regulated at steps that are independent of Pdr1 recruitment.

Altered nucleosome structure at the *PDR5* promoter region in *elm1*Δ strains: Our previous micrococcal nuclease (MNase) mapping of *PDR5* nucleosome structure in *PDR1* and *pdr1-3* strains demonstrated that changes in *PDR5* transcription levels were associated with alterations

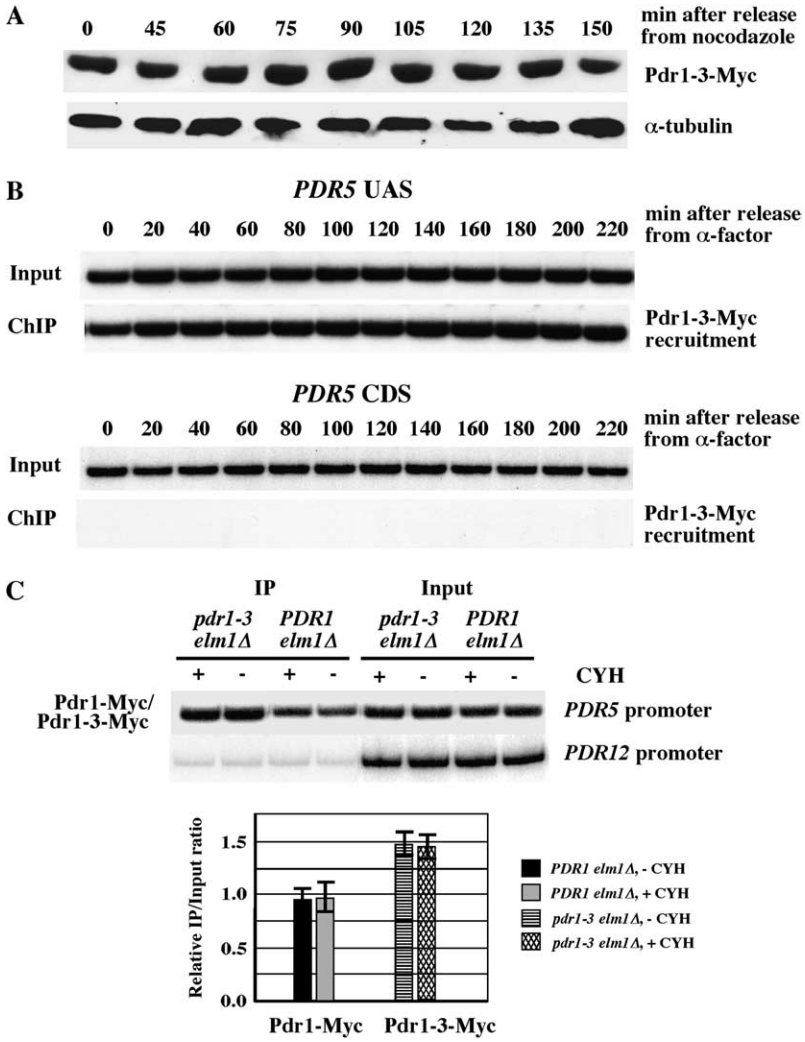

FIGURE 7.—Recruitment of the Pdr1 activator to the *PDR5* promoter was independent of cell cycle progression and *ELM1*. (A) Western blot of Myc-tagged Pdr1-3 activator showed constant levels during the cell cycle. The synchronization and release procedures were done as described in Figure 3A. The same blot was also probed with antibodies against α-tubulin as a control. (B) ChIP using antibodies against Myc-tagged Pdr1-3 showed constitutive recruitment of the Myc-tagged Pdr1-3 activator to the UAS region of the *PDR5* promoter. No recruitment to the CDSs of *PDR5* was observed. The tagged strain was synchronized in YPD medium containing 3 μg/ml α-factor and then released at the indicated time points. The amount of whole-cell lysate used in the input PCR (Input) was 1/200 of that used for ChIP. (C) Myc-tagged Pdr1 and Pdr1-3 activators were constitutively recruited to the *PDR5* UAS in the strains bearing the *elm1*Δ allele. (Top) Recruitment of C-terminally Myc-tagged activators Pdr1 and Pdr1-3 to the UAS of the *PDR5* promoter was analyzed by ChIP. PCR was used to amplify *PDR5* promoter DNA recovered in the anti-Myc antibody immunoprecipitation (IP) products. The recruitment signals of Pdr1 or Pdr1-3 to the *PDR12* promoter served as negative controls. (Bottom) The recruitment signals of Pdr1 or Pdr1-3 to *PDR5* UAS were presented as relative IP/input ratio by a histogram. The histogram does not take into account that the input PCR used 1/200 the amount of the whole-cell lysate than that used for ChIP. Error bars are standard deviations among three independent experiments.

in *PDR5* nucleosome structure even though Pdr1 was constitutively bound (GAO *et al.* 2004; MILGROM *et al.* 2005). This is consistent with the notion that regulation of chromatin structure plays a major role in gene activation (reviewed by BERNSTEIN and ALLIS 2005; BOEGER *et al.* 2005). As the *elm1*Δ allele drastically reduced *PDR5* transcription (Figures 4D and 5B), we next examined the nucleosome structure at the *PDR5* promoter region and compared *pdr1-3* and *pdr1-3 elm1*Δ strains under either noninduced or CYH-induced conditions (Figure 8A). In both *pdr1-3* and *pdr1-3 elm1*Δ strains, CYH induction did not significantly change the pattern or intensities of bands corresponding to MNase hypersensitive sites throughout the *PDR5* promoter region (Figure 8A, compare − and + CYH). It is worth noting that, unlike *PDR5* coding sequences, the absence of typical well-positioned nucleosomes in the *PDR5* UAS region may reflect the GC-rich nature of *PDR5* PDREs sequences (GAO *et al.* 2004). In contrast, the *pdr1-3 elm1*Δ strain showed significant reductions in the intensity of several bands (marked with asterisks) clustered in the region from −700 to −900, extending to ∼−1100 (Figure 8A, labels on the right) relative to the transcription start site (+1). The loss of other bands marked from −900 to −1100 in the *pdr1-3 elm1*Δ strain may reflect restoration of positioned nucleosome structure in this region due to reduced *PDR5* transcription. These nucleosomal alterations were unexpected because this region is located well upstream of the known Pdr1-binding sites (PDREs) and TATA box, and there were no significant differences within the PDREs or TATA region for the *pdr1-3* and *pdr1-3 elm1*Δ strains (Figure 8A). To test the generality of these observations, we performed a set of MNase mapping experiments comparing *PDR1* with *PDR1 elm1*Δ strains and found consistent results (data not shown).

We then investigated whether *PDR1* and/or *PDR3* are required for regulation of nucleosome structure upstream of the PDREs. We examined the latter by using a set of isogenic strains: wild type, *pdr1*Δ, *pdr3*Δ, and *pdr1*Δ *pdr3*Δ (WCS265–WCS268, Table 1). As expected, a strong band located close to the TATA box was observed in the wild-type strain (Figure 8B; GAO *et al.* 2004). Neither *pdr1*Δ nor *pdr3*Δ alone significantly

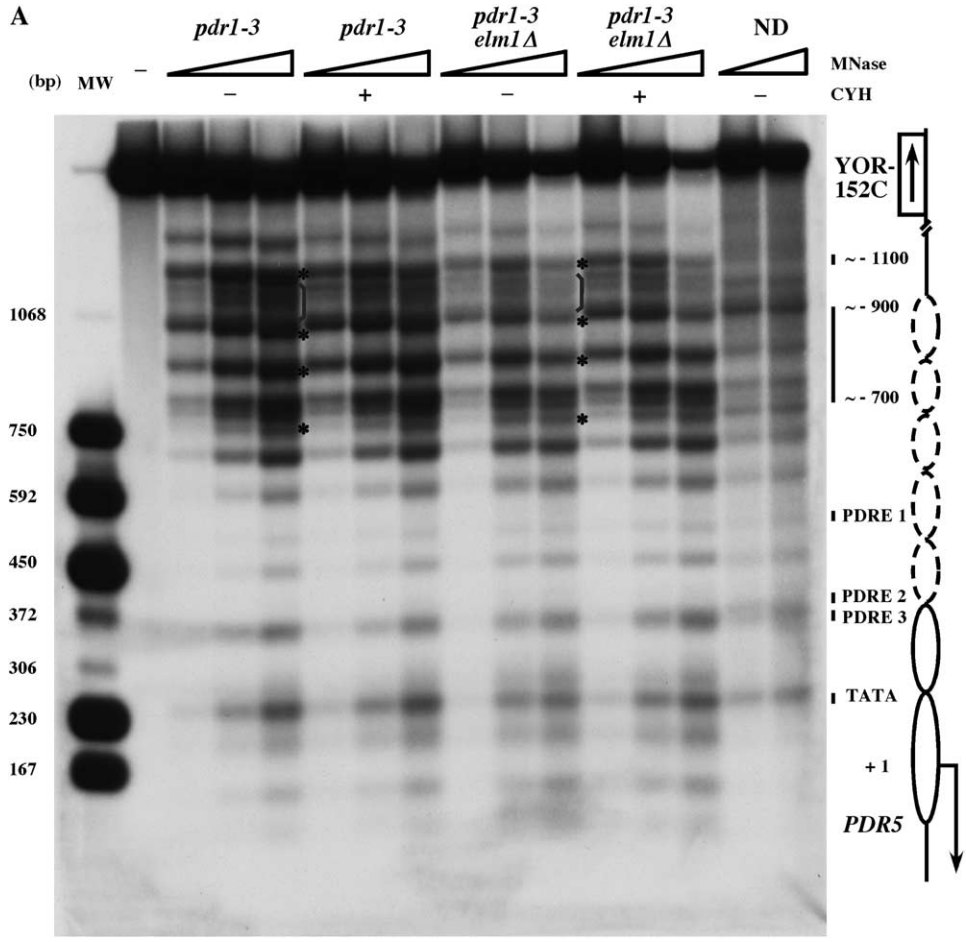

FIGURE 8.—Location of altered chromatin structure of the *PDR5* promoter in the *elm1*Δ and *pdr1*Δ *pdr3*Δ strains. (A) Analysis of MNase susceptibility of the *PDR5* promoter region in *pdr1-3 vs. pdr1-3 elm1*Δ strains, with and without CYH induction. Distinctive differences between *pdr1-3* and *pdr1-3 elm1*Δ strains in the hypersensitive sites located at ~700–~1100 bp upstream of the transcription start site are marked with asterisks or brackets. The *PDR5* transcription start site is marked as +1. The increasing concentrations of MNase marked by triangles represent 25, 50, and 100 units/ml of the enzyme in MNase digestion. ND, naked DNA. MNase (10 units) was used to digest naked DNA. Open ovals depict positioned nucleosome structures, whereas dotted-line ovals depict more dynamic and less well-positioned nucleosome structures. Adjacent ORF YOR152C (768 bp), oriented in the opposite direction of *PDR5*, was indicated in a different scale. (B) Analysis of MNase susceptibility of the upstream *PDR5* promoter region in the wild type (WT), *pdr1*Δ, *pdr3*Δ, and *pdr1*Δ *pdr3*Δ strains without CYH induction. Differences in the intensity of bands corresponding to MNase hypersensitive sites located at the established *PDR5* promoter and coding sequences are marked with #'s and a bracket, respectively; asterisks mark sites located farther upstream. MNase was used at 25 and 50 units. Open and dotted-line ovals were as defined in A. In B, *PDR5* is mapped in the opposite direction of that in A for better resolution of the region encompassing ~ −700 to −900. More details are described in MATERIALS AND METHODS and previously (GAO *et al.* 2004). (C) Diagram depicting the construction of the *pdr5 promoter* Δ*400* strain, which harbors a *TRP1* replacement of the sequences located between nucleotides −726 and −1123 relative to the *PDR5* transcription start site. The arrows denote the directions of the transcription of the *PDR5* (4533 bp), *TRP1* (1049 bp), and open reading frame YOR152C (768 bp). The intergenic region iYOR152C containing the promoter of YOR152C was indicated. (Top inset) Northern blot analysis of *PDR5* mRNA in wild-type strain and the *pdr5 promoter* Δ*400* strain, which indicated decreased *PDR5* transcription in the *pdr5 promoter* Δ*400* strain under both noninduced and CYH-induced conditions. (Bottom inset) Agar plate drug resistance assay for the wild-type and *pdr5 promoter* Δ*400* strains on YPD in the absence or presence of CYH.

changed the *PDR5* promoter region (including TATA box and PDREs), consistent with overlapping roles of Pdr1 and Pdr3 as transcriptional activators (WOLFGER *et al.* 1997). Interestingly, a *pdr1*Δ *pdr3*Δ double deletion resulted in changes not only in the *PDR5* promoter (Figure 8B, #) and coding sequences (bracketed in Figure 8B) as expected, but also in the region upstream of the PDREs, including sequences from −700 to −900 (Figure 8B, asterisks). The increased site-specific MNase digestion presumably reflects less dynamic nucleosome structure in the absence of *PDR1* and *PDR3* (Figure 8B). These data indicate that Pdr1 or Pdr3 is required for regulation of the *PDR5* nucleosome structure upstream of the PDREs, corresponding to the region where the *elm1*Δ strain exhibited altered nucleosome structure. However, Myc-tagged Pdr1 was not recruited to the −700 to −900 region of *PDR5* promoter (data not shown). This raises the possibility that PDREs occupied by Pdr1 and Pdr3 propagate altered nucleosome structure from their binding sites to sequences farther upstream. Such a long-distance effect on nucleosomal structure resulting from changes in the interactions of transcription factors and DNA has been reported previously (FLEMING and PENNINGS 2001).

We then analyzed whether sequences upstream of the PDREs affect *PDR5* transcription. We engineered a wild-type strain with the sequences from ~ −700 to ~ −1100 replaced by *TRP1* (diagrammed in Figure 8C, the resulting strain named *pdr5 promoter* Δ*400* strain). *PDR5* transcription in the *pdr5 promoter* Δ*400* strain was significantly reduced compared to its parental strain *PDR1* under both noninduced and induced conditions. As expected, the

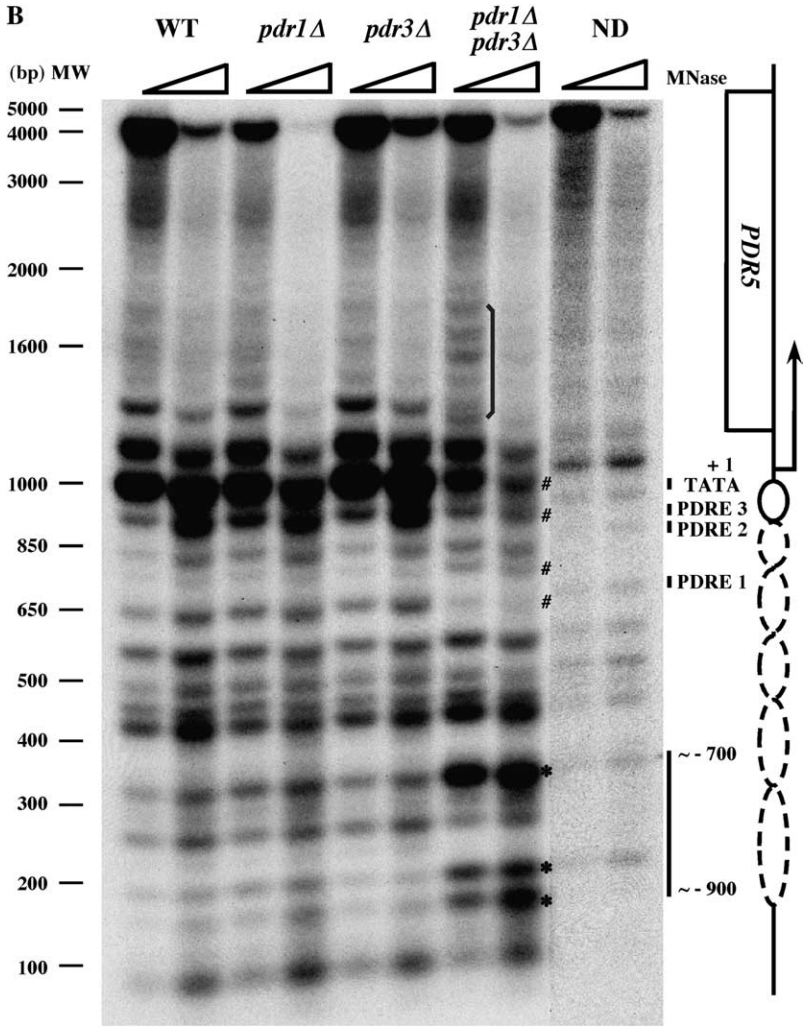

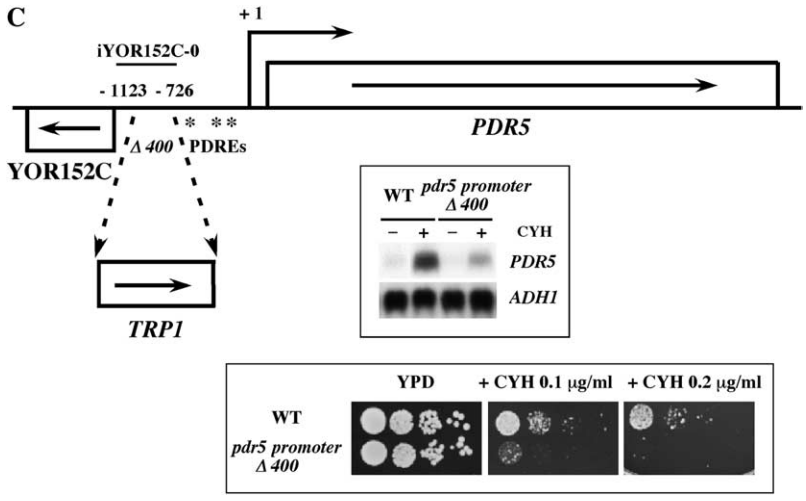

FIGURE 8.—*Continued.*

pdr5 promoter Δ400 strain is hypersensitive to CYH (Figure 8C). Not surprisingly, a reduced mRNA level of adjacent open reading frame YOR152C was detected in the *pdr5 promoter Δ400* strain; however, deletion of YOR152C in *PDR1* or *pdr1-3* strains did not change their resistance to drugs (data not shown). Taken together, the data presented in Figure 8 identify sequences important for *PDR5* transcription located considerably upstream of the PDREs. Significantly, the nucleosome structure in this region requires *ELM1* as well as *PDR1/PDR3*.

We then tested whether Elm1 directly regulates *PDR5* transcription. We analyzed the recruitment of Myc-tagged

Elm1 onto the *PDR5* promoter and upstream region (up to and including the promoter of adjacent ORF YPR152C) in the *PDR1* and *pdr1-3* strains. In Figure 8C, the promoter region of ORF YPR152C is depicted as iYOR152-0 (Horak *et al.* 2002; Harbison *et al.* 2004). No Elm1-Myc recruitment was detected on the promoter of either *PDR5* or YOR152C (data not shown). This result is not surprising since Elm1 has been shown to be located primarily, if not exclusively, at the bud neck between mother and daughter cells (Huh *et al.* 2003; Thomas *et al.* 2003). It is worth noting that the Myc-tagged Elm1 is functional in these strains on the basis of their normal cell morphology and growth. Therefore, the results suggest an indirect mechanism for Elm1 affecting *PDR5* transcription.

DISCUSSION

In this study, we investigated the regulation of multidrug resistance involving the transcription of *PDR5*. We show that in a *pdr1-3* strain, increased *PDR5* transcription (Gao *et al.* 2004) correlates with increased levels of Pdr5 protein (Figure 1). These results are consistent with microarray analysis, revealing *PDR5* as the major target in a *pdr1-3* strain (DeRisi *et al.* 2000). These results also underscore the notion that transcriptional upregulation is the predominant mechanism for development of yeast drug resistance. This is distinct from the development of mammalian drug resistance in which mechanisms unrelated to transcription, such as gene amplification, play a crucial role in addition to transcriptional regulation (Gottesman *et al.* 1995).

Employing the anticancer drug doxorubicin as a substrate, we demonstrated that cellular doxorubicin elimination follows zero-order kinetics (Figure 2D and Table 2), indicative of catalysis; that is, its rate depends on the concentration of the catalyst (ABC transporters in this case) and not on the reactant (cellular doxorubicin concentration) (Tinoco *et al.* 1985). These findings are similar to the elimination of viblastine via P-glycoprotein, in which the results fit to Michaelis–Menten kinetics, $V = V_{max}[S]/K + [S]$. When the concentration of substrates like vinblastine or doxorubicin (S) exceeds K and the rate (V) approaches V_{max}, the efflux catalyzed by P-glycoprotein or Pdr5 will show zero-order kinetics and the number of transporters becomes limiting (Ambudkar *et al.* 1997). Such kinetics ensures efficient and almost complete cellular detoxification.

We demonstrated a striking inverse correlation between *PDR5* mRNA levels and cellular doxorubicin accumulation during cell cycle progression (Figure 3). In these experiments, cellular doxorubicin at any given time point reflected the collective activities of many drug transporters. However, it became apparent that Pdr5 was the most important cell-cycle-regulated transporter, at least for doxorubicin and CYH. It is worth noting that, with equivalent treatments, doxorubicin content in the *pdr1-3* cells during the G_1 phase (2.0 pmol/10^7 cells, Figure 3B) was higher than that in the unsynchronized *PDR1* cells (~1.0 pmol/10^7 cells, Figure 2C, 15 min). Therefore, G_1-synchronized *pdr1-3* cells exhibited even greater sensitivity than unsynchronized *PDR1* cells with respect to detoxification of doxorubicin. The generality of this observation for different drugs and to what degree cell-cycle-dependent drug sensitivity occurs in pathogenic yeast and cancer cells remain to be thoroughly investigated.

We searched for the most appropriate substrate to measure Pdr5 efflux in the various mutants. Ideally, an inert substrate is preferable. Fluconazole, an inhibitor of ergosterol biosynthesis (Kontoyiannis *et al.* 1999), was separated on HPLC and detected by absorbance. However, the detection sensitivity was too low (~5 nmol). Doxorubicin, on the other hand, was detected by fluorescence; its lowest detection limit (with a signal-to-noise ratio >3) was <5 pmol.

The doxorubicin-induced DNA damage results in cell cycle arrest at the G_2/M phase (Siu *et al.* 1999). This process is mediated by inhibiting dephosphorylation of the $p34^{cdc2}$ kinase (mammalian homolog of the *S. cerevisiae* Cdc28) and by inducing cyclin B1 accumulation (Ling *et al.* 1996). Since doxorubicin effect of the cell cycle is expected to be similar in all strains studied, the loss of doxorubicin efflux in *pdr1-3 cla4*Δ, *pdr1-3 elm1*Δ, and *pdr1-3 cdc29-C127Y* strains (Table 2) reflects primarily the effects of the genetic mutations on G_2/M transition.

We provided several lines of evidence that establish a genetic connection between *PDR5* and *ELM1* or *ELM1*-related genes required for proper mitotic progression. First, cells harboring *elm1*Δ exhibit G_2/M delay, reduction of *PDR5* transcription, and loss of CYH resistance (Figures 4 and 5). Second, epistasis analysis indicates that although the *elm1*Δ mutation does not increase CYH susceptibility of the *pdr1-3 pdr5*Δ strain, the *pdr1-3 pdr5*Δ *elm1*Δ strain becomes more sensitive to CYH than the *pdr1-3 elm1*Δ strain (Figure 4D). These data suggest that *ELM1* functions as an upstream regulator of the *PDR5*-mediated CYH resistance. Third, mutations of genes causing defective mitotic progression decrease *PDR5* transcription and CYH resistance (Figures 5 and 6). Fourth, doxorubicin efflux in the *pdr1-3 elm1*Δ, *pdr1-3 cla4*Δ, and *pdr1-3 cdc28-C127Y* strains is virtually undetectable (Table 2). The drug efflux rates in these strains are ~2 orders of magnitude lower than that in the *pdr1-3* strain (Table 2). These data provide a quantitative estimate of the functional consequences of downregulating drug transporter genes in these mutants. The expression of *PDR5* and perhaps other cell-cycle-regulated transporter genes is severely diminished by these mutations. This finding is consistent with the genomewide analysis showing that the expression of several ABC transporter genes (including *TPO1*, *TPO2*,

TPO3, and *TPO4*) peaks during the M phase, while the transcription of other well-established transporter genes peaks at other stages of the cell cycle (*e.g.*, *SNQ2* peaks at G_2 and *FLR1* at S phase) (Spellman *et al.* 1998). Fifth, *elm1*Δ leads to detectable alteration in nucleosome structure upstream of known PDREs at the *PDR5* promoter region (Figure 8). The alteration of *PDR5* nucleosome structure by *elm1*Δ appears independent of the recruitment of Pdr1 to the PDREs (Figure 7). Identification of a new region whose nucleosome structure undergoes conformational changes is consistent with the initial characterization of the *PDR5* promoter, which indicated that sequences of ~1.1 kb upstream of the *PDR5* translation start site were required for maximal *PDR5* expression (Katzmann *et al.* 1996).

We note that the biochemical connection between *ELM1* and *PDR5* transcription is most likely via an indirect mechanism. This conclusion is based on the fact that Elm1 is a key cellular regulatory kinase and predominately located at the bud neck and is not detectable on the *PDR5* promoter by ChIP. The mechanism by which Elm1 regulates the nucleosome structure of the *PDR5* promoter, therefore, remains to be determined. The fact that both Pdr1 and Pdr3 are phosphorylated (Mamnun *et al.* 2002) raises the possibility that phosphorylation of Pdr1/Pdr3 by either Elm1 or its related kinases may affect the activity of Pdr1/Pdr3. In this regard, differential phosphorylation has been proposed to regulate the activity of Gal4 (Mylin *et al.* 1990), the founding member of the Cys_6-Zn(II) DNA-binding transcription factor family to which Pdr1 and Pdr3 belong (Poch 1997). It is interesting to note that the sequences SPVR (amino acids 942–945) and SPLK (amino acids 890–893) of Pdr1 and Pdr3, respectively, are located within the C-terminal transcription activation domains. These are consensus target sequences (S/T-P-X-K/R) for Cdc28 kinase. It is tempting to speculate that Cdc28 could participate in transcriptional regulation of *PDR5* by modulating the activities of constitutively bound Pdr1/Pdr3 activators. Elm1, then, may be linked to Cdc28 activity via regulating Swe1 phosphorylation state during mitosis (Sreenivasan and Kellogg 1999). Consistent with this possibility, a *pdr1-3 elm1*Δ *swe1*Δ strain partially restores a transcriptional defect of *PDR5* observed in the *pdr1-3 elm1*Δ strain (Figure 5B and data not shown). A potential requisite tie among Elm1 (or Cdc28), Pdr1/Pdr3 phosphorylation states, and *PDR5* transcription level remains to be investigated.

The nucleosome structure affected by *elm1*Δ is located ~900 bp upstream of the *PDR5* transcription start site (134 nucleotides upstream of translation start codon ATG). This region encompasses the predicted promoter of the open reading frame YOR152C, which is oriented in the opposite direction of *PDR5* (Figure 8C) and encodes a putative membrane-bound protein of unknown function (Terashima *et al.* 2002). Interestingly, microarray studies indicated that YOR152C mRNA level was significantly upregulated in the *pdr1-3* strain (DeRisi *et al.* 2000). However, deletion of YOR152C did not affect drug resistance of *PDR1* or *pdr1-3* strains (our unpublished data). Further characterization of YOR152C and the divergent promoter between the *PDR5* and YOR152C open reading frames should elucidate molecular aspects of their transcriptional coregulation.

The connection between cell cycle progression and drug transporter gene expression reported here is not unprecedented in other eukaryotes. For instance, in addition to regulation at DNA and mRNA levels, expression of P-glycoprotein is regulated at the protein level. The turnover of P-glycoprotein in multidrug resistant ovarian cells was shown to be cell cycle dependent (Zhang and Ling 2000). Furthermore, it was reported that colon cancer cells overexpressing P-glycoprotein showed a reduced sensitivity to doxorubicin during G_2/M (Toffoli *et al.* 1996). It is therefore suggestive that prior synchronization of drug-resistant cells to the cell cycle stage in which the expression of drug transporters is the lowest (such as G_1 for *PDR5*) could improve the efficacy of treatments of fungal infections and cancers.

The transcription factors that are required for cell-cycle-dependent *PDR5* transcription remain to be explored. Factors known to be recruited to the *PDR5* promoter (*e.g.*, Pdr1, Pdr3, SAGA, Mediator, and SWI/SNF complexes) are potential candidates (Gao *et al.* 2004). Another possibility is the transcription factor Tos4, a known substrate of Cdc28 (Ubersax *et al.* 2003), which regulates cell cycle progression (Iyer *et al.* 2001) and binds to the intergenic region iYOR152C-0 (Horak *et al.* 2002). Moreover, the transcription factor Sok2 also binds to iYOR152C-0 (Harbison *et al.* 2004) and negatively regulates pseudohyphal differentiation/elongated morphology (Pan and Heitman 2000). Interestingly, the iYOR152C-0 region overlaps with the −700 to −1100 region that requires Elm1 and Pdr1/Pdr3 for its proper nucleosome structure (Figure 8).

One intriguing question raised by our studies is why a drug transporter gene such as *PDR5* is specifically expressed during mitosis. It is possible that drug transporter genes regulated by cell-cycle progression may reflect physiological functions of these transporters in addition to their roles as drug transporters (Schmitt and Tampe 2002; Jungwirth and Kuchler 2006). It has been shown that steroids, important components of the cell membrane, are physiological substrates of Pdr5 (Kolaczkowski *et al.* 1996). Moreover, transport of phosphatidylethanolamine is shown to be controlled by the transcription regulators *PDR1* and *PDR3* (Kean *et al.* 1997). As buds grow, biosynthesis and transportation of cell membrane components increase. Drug transporters thus may facilitate proper localization of steroids and other molecules in the newly formed daughter cell membranes. Consistent with this notion, the mammalian P-glycoprotein has been shown to transport, or "flip", short-chain lipids between the leaflets of the cell

membrane (Romsicki and Sharom 2001). Interestingly, the connection among lipid metabolism, drug resistance, and cellular morphogenesis was also demonstrated by the functional analysis of the sphingolipid biosynthetic gene CaIPT1 of *C. albicans*, showing its involvement in both multidrug resistance and cellular morphogenesis (Prasad *et al.* 2005).

In conclusion, we provide genetic, kinetic, and molecular evidence that *ELM1* and functionally related kinase genes are required for multidrug resistance in *S. cerevisiae*. The mechanism for this regulation may include alteration of the nucleosome structure upstream of the *PDR5* PDREs. The proposed mechanism is valid for both *pdr1-3* and *PDR1*.

The authors are grateful to Alan Myers and Daniel Lew for the *cdc28* mutants; Kyung Lee for the septin mutant; and Karl Kuchler, Andre Goffeau, Julius Subik, and Martin Raymond for the *pdr1-3* and *pdr3-2* strains. We thank Bob West and Patty Kane for comments on the manuscript. Constructive input from members of the Yeast Data Club at State the University of NewYork (SUNY) Upstate Medical University and Syracuse University throughout this project is appreciated. A Faculty Development Fund and a Hendrick's Fund provided by SUNY Upstate Medical University to W.-C.W.S. and a grant from the Paige's Butterfly Run to A.-K.S. supported this work.

LITERATURE CITED

Altman, R., and D. Kellogg, 1997 Control of mitotic events by Nap1 and the Gin4 kinase. J. Cell Biol. **138:** 119–130.

Ambudkar, S. V., C. O. Cardarelli, I. Pashinsky and W. D. Stein, 1997 Relation between the turnover number for vinblastine transport and for vinblastine-stimulated ATP hydrolysis by human P-glycoprotein. J. Biol. Chem. **272:** 21160–21166.

Amon, A., 2002 Synchronization procedures. Methods Enzymol. **351:** 457–467.

Asano, S., J. E. Park, K. Sakchaisri, L. R. Yu, S. Song *et al.*, 2005 Concerted mechanism of Swe1/Wee1 regulation by multiple kinases in budding yeast. EMBO J. **24:** 2194–2204.

Bahler, J., 2005 Cell-cycle control of gene expression in budding and fission yeast. Annu. Rev. Genet. **39:** 69–94.

Balzi, E., and A. Goffeau, 1995 Yeast multidrug resistance: the PDR network. J. Bioenerg. Biomembr. **27:** 71–76.

Bauer, B. E., H. Wolfger and K. Kuchler, 1999 Inventory and function of yeast ABC proteins: about sex, stress, pleiotropic drug and heavy metal resistance. Biochim. Biophys. Acta **1461:** 217–236.

Benton, B. K., A. Tinkelenberg, I. Gonzalez and F. R. Cross, 1997 Cla4p, a Saccharomyces cerevisiae Cdc42p-activated kinase involved in cytokinesis, is activated at mitosis. Mol. Cell. Biol. **17:** 5067–5076.

Bernstein, E., and C. D. Allis, 2005 RNA meets chromatin. Genes Dev. **19:** 1635–1655.

Blacketer, M. J., C. M. Koehler, S. G. Coats, A. M. Myers and P. Madaule, 1993 Regulation of dimorphism in Saccharomyces cerevisiae: involvement of the novel protein kinase homolog Elm1p and protein phosphatase 2A. Mol. Cell. Biol. **13:** 5567–5581.

Boeger, H., D. A. Bushnell, R. Davis, J. Griesenbeck, Y. Lorch *et al.*, 2005 Structural basis of eukaryotic gene transcription. FEBS Lett. **579:** 899–903.

Bouquin, N., Y. Barral, R. Courbeyrette, M. Blondel, M. Snyder *et al.*, 2000 Regulation of cytokinesis by the Elm1 protein kinase in Saccharomyces cerevisiae. J. Cell Sci. **113**(Pt. 8): 1435–1445.

Carroll, C. W., R. Altman, D. Schieltz, J. R. Yates and D. Kellogg, 1998 The septins are required for the mitosis-specific activation of the Gin4 kinase. J. Cell Biol. **143:** 709–717.

Carvajal, E., H. B. van den Hazel, A. Cybularz-Kolaczkowska, E. Balzi and A. Goffeau, 1997 Molecular and phenotypic characterization of yeast PDR1 mutants that show hyperactive transcription of various ABC multidrug transporter genes. Mol. Gen. Genet. **256:** 406–415.

Conseil, G., J. M. Perez-Victoria, J. M. Jault, F. Gamarro, A. Goffeau *et al.*, 2001 Protein kinase C effectors bind to multidrug ABC transporters and inhibit their activity. Biochemistry **40:** 2564–2571.

Delahodde, A., T. Delaveau and C. Jacq, 1995 Positive autoregulation of the yeast transcription factor Pdr3p, which is involved in control of drug resistance. Mol. Cell. Biol. **15:** 4043–4051.

Delaveau, T., A. Delahodde, E. Carvajal, J. Subik and C. Jacq, 1994 PDR3, a new yeast regulatory gene, is homologous to PDR1 and controls the multidrug resistance phenomenon. Mol. Gen. Genet. **244:** 501–511.

DeRisi, J., B. van den Hazel, P. Marc, E. Balzi, P. Brown *et al.*, 2000 Genome microarray analysis of transcriptional activation in multidrug resistance yeast mutants. FEBS Lett. **470:** 156–160.

Edgington, N. P., M. J. Blacketer, T. A. Bierwagen and A. M. Myers, 1999 Control of Saccharomyces cerevisiae filamentous growth by cyclin-dependent kinase Cdc28. Mol. Cell. Biol. **19:** 1369–1380.

Egner, R., and K. Kuchler, 1996 The yeast multidrug transporter Pdr5 of the plasma membrane is ubiquitinated prior to endocytosis and degradation in the vacuole. FEBS Lett. **378:** 177–181.

Egner, R., F. E. Rosenthal, A. Kralli, D. Sanglard and K. Kuchler, 1998 Genetic separation of FK506 susceptibility and drug transport in the yeast Pdr5 ATP-binding cassette multidrug resistance transporter. Mol. Biol. Cell **9:** 523–543.

Egner R., B. E. Bauer and K. Kuchler, 2000 The transmembrane domain 10 of the yeast Pdr5p ABC antifungal efflux pump determines both substrate specificity and inhibitor susceptibility. Mol. Microbiol. **35:** 1255–1263.

Eytan, G. D., 2005 Mechanism of multidrug resistance in relation to passive membrane permeation. Biomed. Pharmacother. **59:** 90–97.

Fleming, A. B., and S. Pennings, 2001 Antagonistic remodelling by Swi-Snf and Tup1-Ssn6 of an extensive chromatin region forms the background for FLO1 gene regulation. EMBO J. **20:** 5219–5231.

Fogli, S., R. Danesi, F. Innocenti, A. Di Paolo, G. Bocci *et al.*, 1999 An improved HPLC method for therapeutic drug monitoring of daunorubicin, idarubicin, doxorubicin, epirubicin, and their 13-dihydro metabolites in human plasma. Ther. Drug Monit. **21:** 367–375.

Gao, C., L. Wang, E. Milgrom and W. C. Shen, 2004 On the mechanism of constitutive Pdr1 activator-mediated PDR5 transcription in Saccharomyces cerevisiae: evidence for enhanced recruitment of coactivators and altered nucleosome structures. J. Biol. Chem. **279:** 42677–42686.

Garrett, J. M., 1997 The control of morphogenesis in Saccharomyces cerevisiae by Elm1 kinase is responsive to RAS/cAMP pathway activity and tryptophan availability. Mol. Microbiol. **26:** 809–820.

Gladfelter, A. S., T. R. Zyla and D. J. Lew, 2004 Genetic interactions among regulators of septin organization. Eukaryot. Cell **3:** 847–854.

Golin, J., S. V. Ambudkar, M. M. Gottesman, A. D. Habib, J. Sczepanski *et al.*, 2003 Studies with novel Pdr5p substrates demonstrate a strong size dependence for xenobiotic efflux. J. Biol. Chem. **278:** 5963–5969.

Gottesfeld, J. M., and D. J. Forbes, 1997 Mitotic repression of the transcriptional machinery. Trends Biochem. Sci. **22:** 197–202.

Gottesman, M. M., C. A. Hrycyna, P. V. Schoenlein, U. A. Germann and I. Pastan, 1995 Genetic analysis of the multidrug transporter. Annu. Rev. Genet. **29:** 607–649.

Hallstrom, T. C., and W. S. Moye-Rowley, 2000 Multiple signals from dysfunctional mitochondria activate the pleiotropic drug resistance pathway in Saccharomyces cerevisiae. J. Biol. Chem. **275:** 37347–37356.

Harbison, C. T., D. B. Gordon, T. I. Lee, N. J. Rinaldi, K. D. Macisaac *et al.*, 2004 Transcriptional regulatory code of a eukaryotic genome. Nature **431:** 99–104.

Harisi, R., J. Dudas, F. Timar, G. Pogany, S. Paku *et al.*, 2005 Antiproliferative and antimigratory effects of doxorubicin in human osteosarcoma cells exposed to extracellular matrix. Anticancer Res. **25:** 805–813.

Harlow, E., and D. Lane, 1988 *Antibodies: A Laboratory Manual.* Cold Spring Harbor Laboratory Press, Cold Spring Harbor, NY.

Harvey, S. L., A. Charlet, W. Haas, S. P. Gygi and D. R. Kellogg, 2005 Cdk1-dependent regulation of the mitotic inhibitor Wee1. Cell **122:** 407–420.

Holstege, F. C., E. G. Jennings, J. J. Wyrick, T. I. Lee, C. J. Hengartner *et al.*, 1998 Dissecting the regulatory circuitry of a eukaryotic genome. Cell **95:** 717–728.

Hong, S. P., F. C. Leiper, A. Woods, D. Carling and M. Carlson, 2003 Activation of yeast Snf1 and mammalian AMP-activated protein kinase by upstream kinases. Proc. Natl. Acad. Sci. USA **100:** 8839–8843.

Horak, C. E., N. M. Luscombe, J. Qian, P. Bertone, S. Piccirrillo *et al.*, 2002 Complex transcriptional circuitry at the G1/S transition in Saccharomyces cerevisiae. Genes Dev. **16:** 3017–3033.

Huh, W. K., J. V. Falvo, L. C. Gerke, A. S. Carroll, R. W. Howson *et al.*, 2003 Global analysis of protein localization in budding yeast. Nature **425:** 686–691.

Iyer, V. R., C. E. Horak, C. S. Scafe, D. Botstein, M. Snyder *et al.*, 2001 Genomic binding sites of the yeast cell-cycle transcription factors SBF and MBF. Nature **409:** 533–538.

Jakob, C. A., D. Bodmer, U. Spirig, P. Battig, A. Marcil *et al.*, 2001 Htm1p, a mannosidase-like protein, is involved in glycoprotein degradation in yeast. EMBO Rep. **2:** 423–430.

Jungwirth, H., and K. Kuchler, 2006 Yeast ABC transporters: a tale of sex, stress, drugs and aging. FEBS Lett. **580:** 1131–1138.

Katzmann, D. J., T. C. Hallstrom, Y. Mahe and W. S. Moye-Rowley, 1996 Multiple Pdr1p/Pdr3p binding sites are essential for normal expression of the ATP binding cassette transporter protein-encoding gene PDR5. J. Biol. Chem. **271:** 23049–23054.

Kean, L. S., A. M. Grant, C. Angeletti, Y. Mahe, K. Kuchler *et al.*, 1997 Plasma membrane translocation of fluorescent-labeled phosphatidylethanolamine is controlled by transcription regulators, PDR1 and PDR3. J. Cell Biol. **138:** 255–270.

Koehler, C. M., and A. M. Myers, 1997 Serine-threonine protein kinase activity of Elm1p, a regulator of morphologic differentiation in Saccharomyces cerevisiae. FEBS Lett. **408:** 109–114.

Kolaczkowski, M., M. van der Rest, A. Cybularz-Kolaczkowska, J. P. Soumillion, W. N. Konings *et al.*, 1996 Anticancer drugs, ionophoric peptides, and steroids as substrates of the yeast multidrug transporter Pdr5p. J. Biol. Chem. **271:** 31543–31548.

Kolaczkowska, A., M. Kolaczkowski, A. Delahodde and A. Goffeau, 2002 Functional dissection of Pdr1p, a regulator of multidrug resistance in Saccharomyces cerevisiae. Mol. Genet. Genomics **267:** 96–106.

Kolaczkowski, M., A. Kolaczowska, J. Luczynski, S. Witek and A. Goffeau, 1998 In vivo characterization of the drug resistance profile of the major ABC transporters and other components of the yeast pleiotropic drug resistance network. Microb. Drug Resist. **4:** 143–158.

Kontoyiannis, D. P., N. Sagar and K. D. Hirschi, 1999 Overexpression of Erg11p by the regulatable GAL1 promoter confers fluconazole resistance in Saccharomyces cerevisiae. Antimicrob. Agents Chemother. **43:** 2798–2800.

Kren, A., Y. M. Mamnun, B. E. Bauer, C. Schuller, H. Wolfger *et al.*, 2003 War1p, a novel transcription factor controlling weak acid stress response in yeast. Mol. Cell. Biol. **23:** 1775–1785.

Lawrence, C. W., 1991 Classical mutagenesis techniques. Methods Enzymol. **194:** 273–281.

Lewis, K., 2001 In search of natural substrates and inhibitors of MDR pumps. J. Mol. Microbiol. Biotechnol. **3:** 247–254.

Ling, Y. H., A. K. El-Naggar, W. Priebe and R. Perez-Soler, 1996 Cell cycle-dependent cytotoxicity, G2/M phase arrest, and disruption of p34cdc2/cyclin B1 activity induced by doxorubicin in synchronized P388 cells. Mol. Pharmacol. **49:** 832–41.

Long, J. J., A. Leresche, R. W. Kriwacki and J. M. Gottesfeld, 1998 Repression of TFIIH transcriptional activity and TFIIH-associated cdk7 kinase activity at mitosis. Mol. Cell. Biol. **18:** 1467–1476.

Longtine, M. S., A. McKenzie, III, D. J. Demarini, N. G. Shah, A. Wach *et al.*, 1998 Additional modules for versatile and economical PCR-based gene deletion and modification in Saccharomyces cerevisiae. Yeast **14:** 953–961.

Longtine, M. S., C. L. Theesfeld, J. N. McMillan, E. Weaver, J. R. Pringle *et al.*, 2000 Septin-dependent assembly of a cell cycle-regulatory module in Saccharomyces cerevisiae. Mol. Cell. Biol. **20:** 4049–4061.

Mamnun, Y. M., R. Pandjaitan, Y. Mahe, A. Delahodde and K. Kuchler, 2002 The yeast zinc finger regulators Pdr1p and Pdr3p control pleiotropic drug resistance (PDR) as homo- and heterodimers in vivo. Mol. Microbiol. **46:** 1429–1440.

McMillan, J. N., R. A. Sia, E. S. Bardes and D. J. Lew, 1999 Phosphorylation-independent inhibition of Cdc28p by the tyrosine kinase Swe1p in the morphogenesis checkpoint. Mol. Cell. Biol. **19:** 5981–5990.

McMillan, J. N., C. L. Theesfeld, J. C. Harrison, E. S. Bardes and D. J. Lew, 2002 Determinants of Swe1p degradation in Saccharomyces cerevisiae. Mol. Biol. Cell **13:** 3560–3575.

Mendenhall, M. D., and A. E. Hodge, 1998 Regulation of Cdc28 cyclin-dependent protein kinase activity during the cell cycle of the yeast Saccharomyces cerevisiae. Microbiol. Mol. Biol. Rev. **62:** 1191–1243.

Meyers, S., W. Schauer, E. Balzi, M. Wagner, A. Goffeau *et al.*, 1992 Interaction of the yeast pleiotropic drug resistance genes PDR1 and PDR5. Curr. Genet. **21:** 431–436.

Milgrom, E., R. W. West, Jr., C. Gao and W. C. Shen, 2005 TFIID and Spt-Ada-Gcn5-acetyltransferase functions probed by genome-wide synthetic genetic array analysis using a *Saccharomyces cerevisiae* taf9-ts allele. Genetics **171:** 959–973.

Moye-Rowley, W. S., 2003 Transcriptional control of multidrug resistance in the yeast Saccharomyces. Prog. Nucleic Acid Res. Mol. Biol. **73:** 251–279.

Mylin, L. M., M. Johnston and J. E. Hopper, 1990 Phosphorylated forms of GAL4 are correlated with ability to activate transcription. Mol. Cell. Biol. **10:** 4623–4629.

Nourani, A., D. Papajova, A. Delahodde, C. Jacq and J. Subik, 1997 Clustered amino acid substitutions in the yeast transcription regulator Pdr3p increase pleiotropic drug resistance and identify a new central regulatory domain. Mol. Gen. Genet. **256:** 397–405.

Pan, X., and J. Heitman, 2000 Sok2 regulates yeast pseudohyphal differentiation via a transcription factor cascade that regulates cell-cell adhesion. Mol. Cell. Biol. **20:** 8364–8372.

Piper, P., Y. Mahe, S. Thompson, R. Pandjaitan, C. Holyoak *et al.*, 1998 The pdr12 ABC transporter is required for the development of weak organic acid resistance in yeast. EMBO J. **17:** 4257–4265.

Poch, O., 1997 Conservation of a putative inhibitory domain in the GAL4 family members. Gene **184:** 229–235.

Prasad, T., P. Saini, N. A. Gaur, R. A. Vishwakarma, L. A. Khan *et al.*, 2005 Functional analysis of CaIPT1, a sphingolipid biosynthetic gene involved in multidrug resistance and morphogenesis of Candida albicans. Antimicrob. Agents Chemother. **49:** 3442–3452.

Rogers, B., A. Decottignies, M. Kolaczkowski, E. Carvajal, E. Balzi *et al.*, 2001 The pleitropic drug ABC transporters from Saccharomyces cerevisiae. J. Mol. Microbiol. Biotechnol. **3:** 207–214.

Romsicki, Y., and F. J. Sharom, 2001 Phospholipid flippase activity of the reconstituted P-glycoprotein multidrug transporter. Biochemistry **40:** 6937–6947.

Sakchaisri, K., S. Asano, L. R. Yu, M. J. Shulewitz, C. J. Park *et al.*, 2004 Coupling morphogenesis to mitotic entry. Proc. Natl. Acad. Sci. USA **101:** 4124–4129.

Schmitt, L., and R. Tampe, 2002 Structure and mechanism of ABC transporters. Curr. Opin. Struct. Biol. **12:** 754–760.

Schuetzer-Muehlbauer, M., B. Willinger, R. Egner, G. Ecker and K. Kuchler, 2003 Reversal of antifungal resistance mediated by ABC efflux pumps from Candida albicans functionally expressed in yeast. Int. J. Antimicrob. Agents **22:** 291–300.

Shedden, K., and S. Cooper, 2002 Analysis of cell-cycle gene expression in Saccharomyces cerevisiae using microarrays and multiple synchronization methods. Nucleic Acids Res. **30:** 2920–2929.

Shen, W. C., and M. R. Green, 1997 Yeast TAF(II)145 functions as a core promoter selectivity factor, not a general coactivator. Cell **90:** 615–624.

Sherman, F., 1991 Getting started with yeast. Methods Enzymol. **194:** 3–21.

Sia, R. A., H. A. Herald and D. J. Lew, 1996 Cdc28 tyrosine phosphorylation and the morphogenesis checkpoint in budding yeast. Mol. Biol. Cell **7:** 1657–1666.

Sikorski, R. S., and P. Hieter, 1989 A system of shuttle vectors and yeast host strains designed for efficient manipulation of DNA in *Saccharomyces cerevisiae*. Genetics **122:** 19–27.

Siu, W. Y., C. H. Yam and R. Y. Poon, 1999 G1 versus G2 cell cycle arrest after adriamycin-induced damage in mouse Swiss3T3 cells. FEBS Lett. **461:** 299–305.

Souid, A. K., K. A. Tacka, K. A. Galvan and H. S. Penefsky, 2003 Immediate effects of anticancer drugs on mitochondrial oxygen consumption. Biochem. Pharmacol. **66:** 977–987.

Spellman, P. T., G. Sherlock, M. Q. Zhang, V. R. Iyer, K. Anders *et al.*, 1998 Comprehensive identification of cell cycle-regulated genes of the yeast Saccharomyces cerevisiae by microarray hybridization. Mol. Biol. Cell **9:** 3273–3297.

Sreenivasan, A., and D. Kellogg, 1999 The elm1 kinase functions in a mitotic signaling network in budding yeast. Mol. Cell. Biol. **19:** 7983–7994.

Sreenivasan, A., A. C. Bishop, K. M. Shokat and D. R. Kellogg, 2003 Specific inhibition of Elm1 kinase activity reveals functions required for early G1 events. Mol. Cell. Biol. **23:** 6327–6337.

Sutherland, C. M., S. A. Hawley, R. R. McCartney, A. Leech, M. J. Stark *et al.*, 2003 Elm1p is one of three upstream kinases for the Saccharomyces cerevisiae SNF1 complex. Curr. Biol. **13:** 1299–1305.

Terashima, H., S. Fukuchi, K. Nakai, M. Arisawa, K. Hamada *et al.*, 2002 Sequence-based approach for identification of cell wall proteins in Saccharomyces cerevisiae. Curr. Genet. **40:** 311–316.

Thomas, C. L., M. J. Blacketer, N. P. Edgington and A. M. Myers, 2003 Assembly interdependence among the S. cerevisiae bud neck ring proteins Elm1p, Hsl1p and Cdc12p. Yeast **20:** 813–826.

Tinoco, I., K. Sauer and J. C. Wang, 1985, Kinetics: rates of chemical reactions, pp. 281–282 in *Physical Chemistry: Principles and Selected Applications in Biological Sciences*, Ed. 2. Prentice-Hall, Upper Saddle River, NJ.

Toffoli, G., G. Corona, M. Gigante and M. Boiocchi, 1996 Inhibition of Pgp activity and cell cycle-dependent chemosensitivity to doxorubicin in the multidrug-resistant LoVo human colon cancer cell line. Eur. J. Cancer **32A:** 1591–1597.

Tong, A. H., M. Evangelista, A. B. Parsons, H. Xu, G. D. Bader *et al.*, 2001 Systematic genetic analysis with ordered arrays of yeast deletion mutants. Science **294:** 2364–2368.

Ubersax, J. A., E. L. Woodbury, P. N. Quang, M. Paraz, J. D. Blethrow *et al.*, 2003 Targets of the cyclin-dependent kinase Cdk1. Nature **425:** 859–864.

Walker, S. S., W. C. Shen, J. C. Reese, L. M. Apone and M. R. Green, 1997 Yeast TAF(II)145 required for transcription of G1/S cyclin genes and regulated by the cellular growth state. Cell **90:** 607–614.

Wittenberg, C., and S. I. Reed, 2005 Cell cycle-dependent transcription in yeast: promoters, transcription factors, and transcriptomes. Oncogene **24:** 2746–2755.

Wolfger, H., Y. Mahe, A. Parle-McDermott, A. Delahodde and K. Kuchler, 1997 The yeast ATP binding cassette (ABC) protein genes PDR10 and PDR15 are novel targets for the Pdr1 and Pdr3 transcriptional regulators. FEBS Lett. **418:** 269–274.

Wolfger, H., Y. M. Mamnun and K. Kuchler, 2001 Fungal ABC proteins: pleiotropic drug resistance, stress response and cellular detoxification. Res. Microbiol. **152:** 375–389.

Woods, A., S. R. Johnstone, K. Dickerson, F. C. Leiper, L. G. Fryer *et al.*, 2003 LKB1 is the upstream kinase in the AMP-activated protein kinase cascade. Curr. Biol. **13:** 2004–2008.

Zhang, W., and V. Ling, 2000 Cell-cycle-dependent turnover of P-glycoprotein in multidrug-resistant cells. J. Cell. Physiol. **184:** 17–26.

Communicating editor: A. P. Mitchell